frontiers in Marine Science

ORIGINAL RESEARCH
published: 09 March 2021
doi: 10.3389/fmars.2021.587748

Effectiveness of Fluorescent Viability Assays in Studies of Arctic Cold Seep Foraminifera

*Katarzyna Melaniuk**

Centre for Arctic Gas Hydrate, Environment, and Climate CAGE, Department of Geosciences, UiT The Arctic University of Norway, Tromsø, Norway

Highly negative $\delta^{13}C$ values in fossil foraminifera from methane cold seeps have been proposed to reflect episodes of methane release from gas hydrate dissociation or free gas reservoirs triggered by climatic changes in the past. Because most studies on live foraminifera are based on the presence of Rose Bengal staining, that colors the cytoplasm of both live and recently dead individuals it remains unclear if, and to what extent live foraminifera incorporate methane-derived carbon during biomineralization, or whether the isotopic signature is mostly affected by authigenic overgrowth. In this paper, modern foraminiferal assemblages from a gas hydrate province Vestnesa Ridge (~1,200 m water depth, northeastern Fram Strait) and from Storfjordrenna (~400 m water depth in the western Barents Sea) is presented. By using the fluorescent viability assays CellTracker^{TM} Green (CTG) CMFDA and CellHunt Green (CHG) together with conventional Rose Bengal, it was possible to examine live and recently dead foraminifera separately. Metabolically active foraminifera were shown to inhabit methane-enriched sediments at both investigated locations. The benthic foraminiferal faunas were dominated by common Arctic species such as *Melonis barleeanus*, *Cassidulina neoteretis*, and *Nonionellina labradorica*. The combined usage of the fluorescence probe and Rose Bengal revealed only minor shifts in species compositions and differences in ratios between live and recently dead foraminifera from Storfjordrenna. There was no clear evidence that methane significantly affected the $\delta^{13}C$ signature of the calcite of living specimens.

Keywords: CellTracker^{TM} Green CMFDA, Rose Bengal, gas hydrate, Vestnesa Ridge, Storfjordrenna, cold seep, Arctic

OPEN ACCESS

Edited by:
Daniela Zeppilli, Institut Français de Recherche pour l'Exploitation de la Mer (IFREMER), France

Reviewed by:
Clara F. Rodrigues, University of Aveiro, Portugal
Alessandra Asioli, Institute of Marine Sciences (CNR), Italy

***Correspondence:**
Katarzyna Melaniuk
Katarzyna.Melaniuk@uit.no

Specialty section:
This article was submitted to Deep-Sea Environments and Ecology, a section of the journal Frontiers in Marine Science

Received: *27 July 2020*
Accepted: *15 February 2021*
Published: *09 March 2021*

Citation:
Melaniuk K (2021) Effectiveness of Fluorescent Viability Assays in Studies of Arctic Cold Seep Foraminifera. Front. Mar. Sci. 8:587748. doi: 10.3389/fmars.2021.587748

INTRODUCTION

Due to the present climate warming, the Arctic region is undergoing remarkably rapid environmental changes, termed the Arctic amplification (IPCC, 2013; Box et al., 2019). The increase in global temperature and atmospheric CO_2 has severe consequences for the Arctic Ocean, causing among others ocean acidification (Amap Assessment, 2018), loss of sea ice (Stroeve et al., 2012), and increase in primary production (Arrigo and van Dijken, 2011). The ocean warming also impose

a high risk of release of methane from geological reservoirs (IPCC, 2007; Phrampus and Hornbach, 2012) as large amounts of methane are stored on Arctic continental margins in the form of pressure-temperature sensitive gas hydrates (e.g., Maslin et al., 2010; Ruppel and Kessler, 2017). Gas hydrate is a widespread, ice-like substance formed when water and methane or other hydrocarbon gases combine in marine sediments under high pressure (3–5 MPa) and temperatures below ∼25°C (e.g., Kvenvolden, 1993). Pressure release and/or increase in temperature can cause destabilization of gas hydrate reservoirs, resulting in a release of free methane gas into the sediment and/or water column (e.g., Archer et al., 2009; Maslin et al., 2010). Several studies have implied a link between the release of methane from geological reservoirs and climate change during the Quaternary and the Paleocene periods (e.g., Wefer et al., 1994; Dickens et al., 1997; Smith et al., 2001). It is feared that ongoing climate change can trigger destabilization of gas hydrate reservoirs and methane release into the water column and eventually to atmosphere (Ruppel and Kessler, 2017). Therefore, it is crucial to understand the fate of methane in marine sediments in order to understand the potential impact of methane release to future climate and Arctic ecosystems.

For the last decades, the carbon isotopic signature $\delta^{13}C$ of benthic foraminifera has been commonly used as a proxy in the reconstruction of productivity and origin and ventilation of water masses in the past (e.g., Gooday, 1994, 2003; Smart et al., 1994; Rohling and Cooke, 1999; Murray, 2006; Ravelo and Hillaire-Marcel, 2007). Recent studies have shown that the $\delta^{13}C$ incorporated into the calcareous ($CaCO_3$) tests of benthic foraminifera can record episodes of release of methane in the past (e.g., Torres et al., 2003; Millo et al., 2005; Martin et al., 2010; Schneider et al., 2017; Sztybor and Rasmussen, 2017). The $\delta^{13}C$ in the shells of some fossil benthic foraminifera can be lower than −10‰ (e.g., Hill et al., 2004; Schneider et al., 2017; Sztybor and Rasmussen, 2017), while the signature of calcite of living foraminifera generally do not exceed −7.5‰ (Mackensen et al., 2006; Wollenburg et al., 2015), it remains unclear if, and to what extent live benthic foraminifera incorporate methane-derived carbon during biomineralization, or whether the isotopic signature is mostly affected by authigenic overgrowth from carbonate precipitation.

Modern methane cold seeps can provide valuable information about changes in seepage intensity and the possible effects of methane seepage on the distribution patterns of live foraminifera and the isotopic composition of their tests. The $\delta^{13}C$ of calcareous benthic foraminifera is determined by species-specific vital effects (i.e., intracellular metabolic processes; e.g., Grossman, 1987; McCorkle et al., 1990; Mackensen et al., 2006) and their microhabitat (e.g., sedimentary organic matter, dissolved inorganic carbon content, temperature, and re-mineralization; e.g., McCorkle et al., 1985; Fontanier et al., 2006). Within cold seeps, the release of methane from the seafloor is partly controlled by sulfate-dependent anaerobic oxidation of methane (AOM) and aerobic methane oxidation (MOx; Treude et al., 2007; Knittel and Boetius, 2009). Thus, as a product of these microbial activities, ^{13}C-depleted carbon is released in the form of carbon dioxide (CO_2) or bicarbonate (HCO_3^{2-}), causing changes in the carbon isotopic signature of pore water i.e., changes in the microhabitat (e.g., Whiticar, 1999; Rathburn et al., 2003; Treude et al., 2007).

Since benthic foraminifera construct their tests by incorporating carbon from the surrounding pore water or bottom water and from the intracellular storage of inorganic carbon (e.g., de Nooijer et al., 2009; Toyofuku et al., 2017), the foraminiferal calcite supposedly records the isotopic signal of ambient waters (i.e., pore water or interstitial water in which the foraminifera live) at the time of calcification (e.g., Rathburn et al., 2003; Panieri and Sen Gupta, 2008). Alternatively, foraminifera might absorb the ^{13}C-depleted carbon *via* the food web (Panieri, 2006) or by feeding on, or living in symbiosis with, methanotrophic bacteria, as suggested by Hill et al. (2004). Some studies show that the $\delta^{13}C$ measured in tests of living foraminifera collected from active seeps are not markedly lower than those from non-seep sites, indicating that living foraminifera might not be able to record the episodes of methane release (e.g., Rathburn et al., 2003; Torres et al., 2003; Etiope et al., 2014; Herguera et al., 2014; Dessandier et al., 2020). Simultaneously, numerous other studies indicate that methane has an effect on isotopic signatures of "live" foraminifera (Rose Bengal stained; e.g., Hill et al., 2004; Mackensen et al., 2006; Panieri, 2006; Wollenburg and Mackensen, 2009; Wollenburg et al., 2015).

Studies of live foraminiferal assemblages are commonly based on Rose Bengal staining, presumably marking specimens that were alive at the sampling time. Stained specimens can include both live and recently dead individuals (Bernhard et al., 2006; Figueira et al., 2012) thus, it is still not clear if live foraminifera have recorded the ^{13}C signal that comes from incorporation of carbon from methane in their shells during calcification. Compared to the conventional Rose Bengal, the CellTracker^{TM} Green (CTG) CMFDA (5-chloromethylfluorescein diacetate; Thermo Fisher Scientific) and CellHunt Green (CHG) (SETAREH biotech, LLC) probes are reactive with internal cell components and gives a green-fluorescent coloring of the cytoplasm, indicating metabolically active foraminiferal specimens. The combined usage of the fluorogenic probes together with the Rose Bengal staining can be used to separate live foraminifera from recently dead individuals, and thus be a useful tool to build up a more detailed picture of benthic foraminiferal distribution patterns and ecology. It might be especially useful in studies of heterogeneous and variable environments such as cold seeps, which depend on the highly variable flux of methane and can evolve and change rapidly over time (Levin, 2005; Cordes et al., 2006; Åström et al., 2020).

This paper presents results of a study of live benthic foraminifera from a gas hydrate province on Vestnesa Ridge (∼1,200 m water depth; western Svalbard margin) and from gas hydrate "pingo" structures from Storfjordrenna (∼400 m water depth) in the western Barents Sea (**Figure 1**). The aims of the study are to (1) identify species compositions of the benthic foraminiferal faunas in these Arctic methane seeps and (2) to compare the carbon isotopic signature ($\delta^{13}C$) in the tests of

metabolically active (CTG or CHG labeled) foraminifera, with Rose Bengal stained and with unstained tests (empty tests), to determine if methane seepage has any significant effects on the isotopic signatures of calcite of live benthic foraminifera.

MATERIALS AND METHODS

Study Area

Vestnesa Ridge is located northwest of Svalbard in the eastern Fram Strait and is an approximately 100 km long sediment drift at water depths of ∼1,200–1,300 m. The Fram Strait forms the gateway between the North Atlantic Ocean and the Arctic Ocean. This region is characterized by large annual fluctuations in sea-ice cover. Relatively warm (3–6°C), saline (S < 35.4 psu), and nutrient-rich Atlantic water pass through the Fram Strait into the Arctic Ocean carried by the West Spitzbergen Current (WSC) (e.g., Manley, 1995; Rudels et al., 2000; Walczowski et al., 2005). The southwestern part of the Vestnesa Ridge is characterized by the presence of several active pockmarks (i.e., shallow seabed depressions) where methane-rich fluids seep from gas hydrate and free gas reservoirs (Bünz et al., 2012; **Figure 1B**). The most active pockmarks, "Lomvi" and "Lunde," are approximately 10–15 m deep depressions with diameters

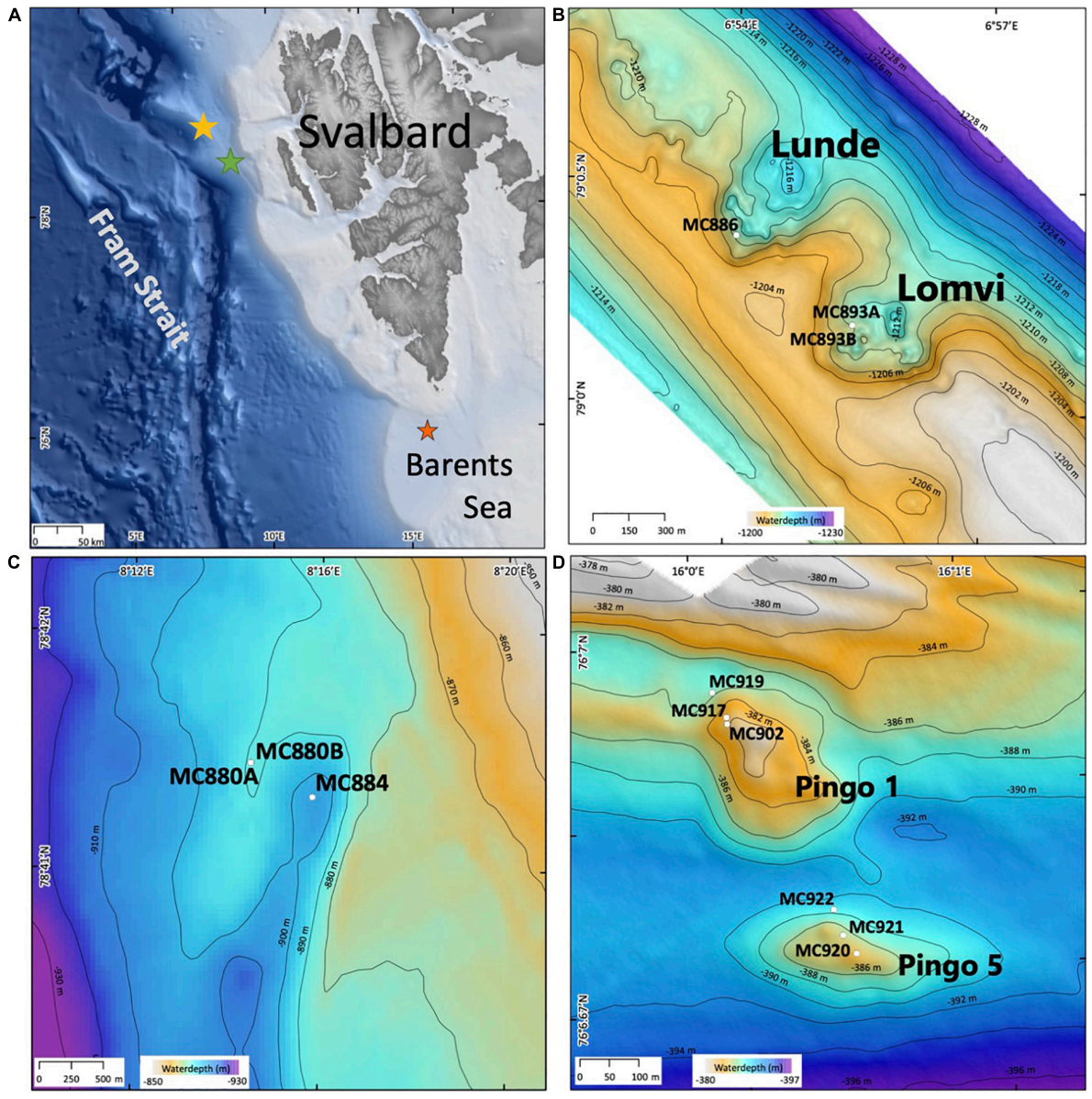

FIGURE 1 | Maps showing **(A)** sampling location, indicated by stars: yellow- Vestnesa Ridge; green- Control site 7,808; orange- Storfjordrenna pingos; **(B)** bathymetry of Vestnesa Ridge (swath bathymetry from Hustoft et al., 2009); control site **(C)** and bathymetry of Storfjordrenna pingos [**(D)**; swath bathymetry from Serov et al. (2017)].

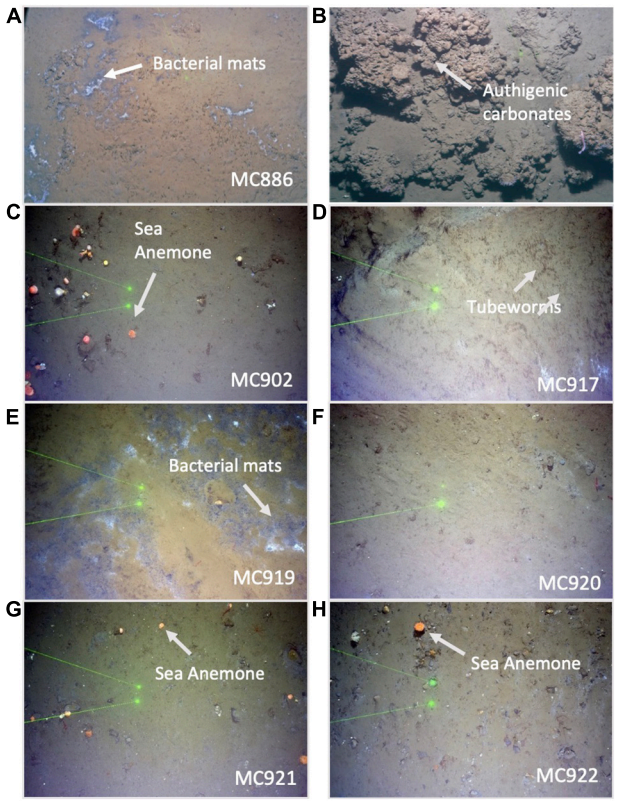

FIGURE 2 | Seafloor images from the Vestnesa Ridge MC886 Lunde pockmark, MC893 Lomvi pockmark showing gray bacterial mats **(A)** and authigenic carbonates **(B)**, and from Storfjordrenna pingos site from active site gas hydrate pingo 1 (GHP1; MC902—MC919) showing tubeworms **(D)**, gray bacterial mats **(E)** and sea anemones **(C)**, and from the inactive site GHP 5 (MC920—MC922) showing sea anemones **(G,H)**. Distance between laser dots (green dots) = 20 cm. **(F)** regular marine sediment.

of 400–600 m. The TowCam−guided multicore investigation of the Vestnesa Ridge shows heterogeneity of the site and presence of macrofauna and seafloor structures associated with the occurrence of methane seepage. These include, e.g., bacterial mats and tubeworm fields (*Siboglinidae*) within the Lunde pockmark, and Methane-Derived Authigenic Carbonate (MDAC) outcrops at the seafloor within the Lomvi pockmark (e.g., Sztybor and Rasmussen, 2017; Åström et al., 2018; **Figure 2**). The $\delta^{13}C_{DIC}$ values of pore water for the Lomvi pockmark have been reported to range between −25.1 and −37.7‰ and for the Lunde pockmark −22.4‰ to −39.4‰ in surface sediments (Dessandier et al., 2019).

The Storfjordrenna hydrate mound "pingo" area is located ∼400 m water depth on the Arctic continental shelf, south of the Svalbard archipelago in the north-western Barents Sea (**Figure 1D**). Similar to the Vestnesa Ridge, Storfjordrenna is under influence of relatively warm Atlantic water (Loeng, 1991). The area is characterized by five gas hydrates mounds (pingo-like features) spread within an area of 2 km^2. The gas hydrate pingos (GHPs) are between 8 and 12 m high, with diameters between 280 and 450 m. Four of the five GHPs are presently active and show active methane seepage in the form of acoustically detected gas/bubble streams (i.e., acoustic flares) around the summits and one is in a "post-active stage" and presently inactive (Hong et al., 2017; Serov et al., 2017). Elevated concentrations of methane (mostly of thermogenic origin) have been detected in both sediments and bottom waters at GHP1, and gas hydrates were recovered in sediment cores (Hong et al., 2017; Carrier et al., 2020). The $\delta^{13}C_{DIC}$ values of pore water for the top of GHP1 (MC902) reached −24.2‰ (Dessandier et al., 2020). Seabed images acquired with a Multicorer-TowCam during the CAGE17-2 cruise revealed the presence of white and gray bacterial mats as well as sediments colonized by chemosynthetic *Siboglinidae* tubeworms, biota well known to indicate active hydrocarbon seepage (Niemann et al., 2006; Treude et al., 2007; **Figure 2**). The megafauna community associated with cold seeps has been previously documented at the Storfjordrenna by Åström et al. (2016) and Sen et al. (2018).

Sampling

Sediment samples were collected during the CAGE 15-2 cruise in May 2015 to Vestnesa Ridge from the sites of active methane emission, the Lomvi and Lunde pockmarks, and at site 7,808 located south-east from the Vestnesa Ridge as a control site where no methane seepage occurs (**Figures 1B,C**). During CAGE cruise 17-2 in June 2017 to Storfjordrenna pingo area, several samples were taken from the active gas hydrates pingo (GHP1) along a transect from the top the pingo toward its edge (**Figure 1D**). For comparison, the inactive GHP5 was sampled in a similar manner (**Figure 1D**).

The samples from both Vestnesa Ridge and the pingo area in Storfjordrenna (**Table 1** and **Figure 1**) were collected with a multicorer equipped with six tubes (10 cm diameter) and combined with a Towed Digital Camera (TowCam) developed at the Woods Hole Oceanographic Institution's Multidisciplinary Instrumentation in Support of Oceanographic (MISO) Facility onboard the R/V *Helmer Hanssen*. The live-stream feed from the TowCam system were used to identify the different seafloor environments and to locate active methane vents, authigenic carbonates, and bacterial mats for targeted accurate sampling locations (**Figure 2**).

After recovery, undisturbed cores were selected for this study. The uppermost core section of each selected core was subsampled using a flat spatula slicing the sediment into 1-cm thick, horizontal intervals (0–1, 1–2, and 2–3 cm). Sediment samples from Vestnesa Ridge were processed as follows: One-third of each slice designated for different treatments, (1) labeling with CTG, (2) staining with Rose Bengal, and (3) extraction of dissolved inorganic carbon (DIC) from pore waters. Each sample was transferred into plastic containers (125-ml HDPE). The CTG solution was prepared beforehand as follows: 1.4 ml of DMSO (dimethyl sulfoxide; not anhydrous) was added to 1 mg CTG, mixed gently, and kept in the original plastic vial from the supplier at −20°C. The solution was thawed approximately 20 min before the sampling. CTG was added to 20 ml of seawater sampled in the multicore tube and added to the sediment immediately after sampling and giving a final concentration of

TABLE 1 | Core numbers, location, coordinates, water depths, and dates of sampling.

Core number	Location	Coordinates	Water depth (m)	Sampling date
MC893A and MC893B	Vestnesa Ridge (Lomvi pockmark)	79.18N, 00.44E	1200	20 May 2015
MC886	Vestnesa Ridge (Lunde pockmark)	79.38N, 00.04E	1200	20 May 2015
MC880A and MC880B	Site 7808 (Control site)	78.44N, 00.50E	889	19 May 2015
MC884	Site 7808 (Control site)	78.30N, 00.82E	900	19 May 2015
MC902	Storfjordrenna Active GHP1	76.91N, 16.08E	377	22 June 2017
MC917	Storfjordrenna Active GHP1	76.93N, 16.02E	377	23 June 2017
MC919	Storfjordrenna Active GHP1	76.96N, 15.98E	378	23 June 2017
MC920	Storfjordrenna Inactive GHP5	76.70N, 16.00E	379	23 June 2017
MC921	Storfjordrenna Inactive GHP5	76.72N, 16.40E	380	23 June 2017
MC922	Storfjordrenna Inactive GHP5	76.74N, 16.37E	386	23 June 2017

GHP, gas hydrates pingo.

CTG of 1 μM in seawater (Bernhard et al., 2006). Samples were incubated in a temperature-controlled room at 4°C for approximately 12 h. Rose Bengal solution was made prior to sampling by dissolving Rose Bengal powder in distilled water (2 g/L). The solution was added to the designated sediment samples, agitated gently, and kept in plastic containers (250 ml). Sediment labeled with CTG and stained with Rose Bengal was preserved with 36% formaldehyde (to final concentration 5.5%) and kept at 4°C.

The sediment collected from Storfjordrenna pingo area was treated differently when compared to samples from the Vestnesa Ridge. Each 1-cm slice of sediment taken from GHP multicores was directly transferred into a 125 ml HDPE bottle. The whole sediment was treated with the CHG solution. The CHG solution was prepared beforehand (following the protocol for CTG). Samples were incubated in CHG onboard in a dark, temperature-controlled room at 4°C for approximately 12 h. Hereafter, the samples were preserved in ethanol with final concentration 70%.

Foraminiferal Fauna Analysis

Rose Bengal stained and CTG labeled (i.e., fluorescently labeled) samples from Vestnesa Ridge were washed over a 63-μm sieve using filtered seawater (0.45 μm); the >63 μm fraction was kept in filtered seawater and further analyzed. The fluorescently labeled samples were examined using an epifluorescence-equipped stereomicroscope (Leica MZ FLIII; 485 nm excitation; 520 nm emission). All individuals that fluoresced brightly in at least half of their chambers were considered as live (**Figure 6**). They were picked wet and placed on micropaleontology slides. The Rose Bengal stained samples were examined with reflected-light microscopy using a Zeiss Stemi SV6. All foraminifera that stained dark magenta in at least half of their chambers were picked and mounted on micropaleontology slides (**Figure 3**). All collected foraminifera were sorted by species and counted and identified to species level (**Tables 2**, **3**).

The CHG labeled (i.e., fluorescently labeled) sediment samples from GHPs were processed in the same manner as CTG labeled, except that individuals that did not show any green coloration were subsequently incubated in a Rose Bengal-ethanol solution (2 g/L). After approximately 24 h, samples were re-sieved over a 63-μm sieve. Obtained Rose Bengal stained foraminifera were wet picked (**Figure 3**). Unstained tests have been omitted and not counted in this study.

The density of foraminifera was normalized per unit volume at the number of specimens per 10 cm^3. The Shannon index S(H) of diversity, Evenness index, and Chao1 index (**Tables 2**, **3**) was calculated for each sample. The number of CTG labeled and Rose Bengal stained foraminifera, as well as the CHG labeled and Rose Bengal stained foraminifera, were compared by chi-square testing. Assuming that CHG foraminifera would have stained with Rose Bengal, the number of Rose Bengal stained foraminifera was determined as a sum of CHG labeled (living) and Rose Bengal stained (recently dead) individuals. For our chi-square test, the Rose Bengal stained individuals were treated as the expected values, whereas the CTG or CHG labeled individuals were treated as the observed values; this approach is adapted from Bernhard et al. (2006). The percentage of CHG labeled (living) faunal assemblages from GHP sites were calculated relative to total foraminiferal abundance (CHG labeled + Rose Bengal stained, i.e., foraminifera containing cytoplasm; **Figure 7**). Due to similar properties, further in the text CTG and CHG labeled foraminifera are interchangeably referred to as "fluorescently labeled."

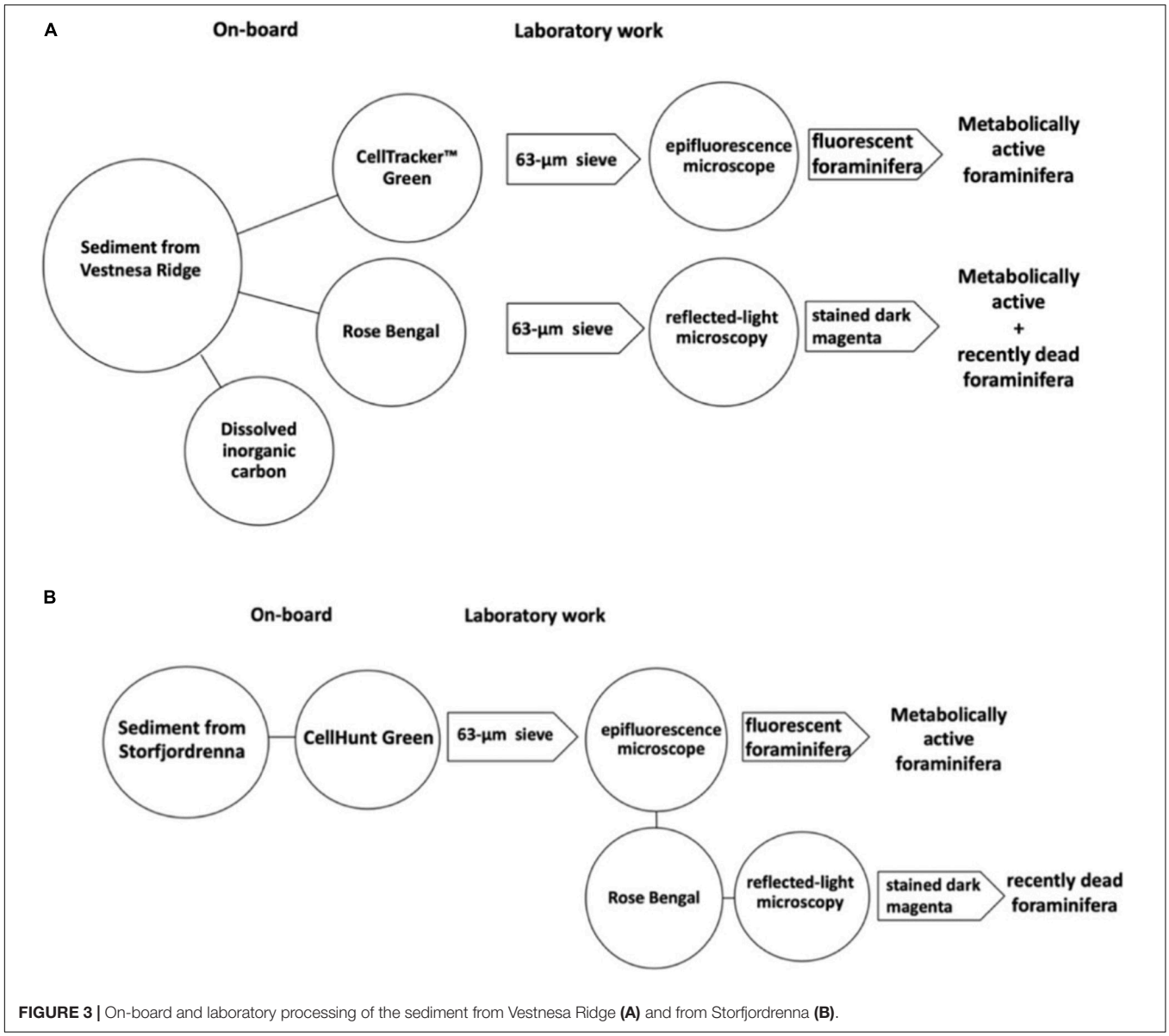

FIGURE 3 | On-board and laboratory processing of the sediment from Vestnesa Ridge **(A)** and from Storfjordrenna **(B)**.

Stable Isotopes Analyses

For carbon ($\delta^{13}C$) stable isotope analyses of Vestnesa Ridge samples, the most numerous individuals of species indicated as a metabolically active (CTG labeled; live) and individuals "live + recently dead" (Rose Bengal stained) were selected. Due to the small size of most specimens, between 8 and 10 specimens of *Melonis barleeanus* and *Cassidulina neoteretis* (when present) and 10 unstained tests of the planktonic foraminiferal species *Neogloboquadrina pachyderma* were picked from each sample. In case of foraminifera from GHPs, $\delta^{13}C$ measurements were performed on metabolically active (CHG labeled) foraminifera and recently dead (Rose Bengal stained) foraminifera of the two most numerous species *M. barleeanus* and *Nonionellina labradorica* (between eight and 10 specimens). Some "dead" (unstained tests) were picked for isotope analyses for comparison. Whenever possible, replicates were processed and analyzed.

Isotopic measurements were performed on a MAT 253 Isotope Ratio Mass Spectrometer (Department of Geosciences, UiT The Arctic University of Norway). Carbon isotopic compositions are expressed in conventional δ notation against the Vienna Pee Dee Belemnite (V-PDB) standard (1.96, −10.21, and −48.95‰ for $\delta^{13}C$) and reported in parts per thousand (per mil, ‰). Analytical precision was estimated to be better than 0.07‰ for $\delta^{13}C$ by measuring the certified standard NBS-19.

RESULTS

Foraminiferal Assemblages

Vestnesa Ridge

Fluorescently labeled (living) individuals were present in the sediment from core MC893A (Lomvi pockmark) at 0–1 cm and

TABLE 2 | Direct counts of CellTracker™ Green labeled foraminifera from all samples.

	Control site									**Vestnesa Ridge**								
Core number	**MC880A**			**MC880B**			**MC884**			**MC886**			**MC893A**			**MC893B**		
Depth (cm)	0–1	1–2	2–3	0–1	1–2	2–3	0–1	1–2	2–3	0–1	1–2	2–3	0–1	1–2	2–3	0–1	1–2	2–3
Cassidulina laevigata	4						1											
Cassidulina neoteretis	22	1		21	7		4	1					13	2				
Cassidulina reniforme				3	1		4						2					
Cibicides lobatulus				3									1	1				
Melonis barleeanus	4	3		6	7		8	7					10	9				
Nonionellina labradorica								3					1					
Pullenia bulloides	1			4			2	5					2					
Total number/sample	31	4		37	15		19	16					29	12				
SD	9,60	1,41		7,7	3,46		2,68	2,584					5,26	4,35				
Number/10 cm^3	11.9	1.5		14.2	5.7		7.7	6.2					11.15	5				
#Taxa	4	2		5	3		5	4					6	3				
Shannon's H index	0.88	0.56		1.03	1.22		1.41	1.21					1.33	0.72				
Evenness index	0.60	0.87		0.70	0.81		0.82	0.84					0.62	0.58				
Chao1 index	4	2		5	3		5	4					6.3	3				

TABLE 3 | Direct counts of Rose Bengal stained foraminifera from all samples.

	Control site									Vestnesa Ridge								
Core number	**MC880A**			**MC880B**			**MC884**			**MC886**			**MC893A**			**MC893B**		
Depth (cm)	0–1	1–2	2–3	0–1	1–2	2–3	0–1	1–2	2–3	0–1	1–2	2–3	0–1	1–2	2–3	0–1	1–2	2–3
Adercotryma glomeratum		3																
Buccella frigida		7		5				1					14	6				
Cassidulina laevigata	1							1	1	1								
Cassidulina neoteretis	44	24		11	12	17	9	13	3				9	2				
Cassidulina reniforme		3		1	1		3	1					8	1	1			
Cibicides lobatulus	4						2	2					2					
Elphidium excavatum									1							3		
Fissurina sp.				2														
Labrospira crassimargo										7								
Lagena sp. 1		1						1										
Lagena sp. 2		1							1				1					
Melonis barleeanus	16			10	31	23	8	28	12	1			52	16	5	16	14	3
Nonionellina labradorica					1	3		1	1				1					
Pullenia bulloides	4	3			2	2	2	8	3	1			1	1		2		
Reophax guttifer		3						4	2					1				
Reophax fusiformis							2						12					
Reophax sp.				2	5	1			1				1	2		7		
Stainforthia loeblichi		1						2		1								
Spiroplectammina earlandi				1						4			1					
Trifarina angulosa	1			2			2											
Triloculina sp.				1			1		2									
Total number/sample	70	46		35	52	46	29	62	27	15			102	29	6	28	14	3
SD	17.83	7.32		3.95	11.70	10.10	3.06	8.34	3.36	2.5			15	5.52	2.82	6.37	0	0
Number/10 cm^3	27	18		13 >4	20	17.6	11.2	23.8	10.4	5.8			39.2	11.2	2.3	10.7	5.4	1.2
#Taxa	6	9		9	6	5	8	11	10	6			11	7	2	4	1	1
Shannon's H index	1.08	1.55		1.79	1.15	1.04	1.80	1.62	1.75	1.43			1.6	1.37	0.45	1.09	0	0
Evenness index	0.55	0.54		0.66	0.52	0.60	0.76	0.48	0.63	0.69			0.44	0.56	0.78	0.74	1	1
Chao1 index	5	12		9.75	6.5	5	8	14.33	13.33	12			16	8	2	4	1	1

1–2 cm core depths, but not in the 2–3 cm interval. None of the individuals in cores MC886 and MC893B were metabolically active. At the control site, fluorescently labeled foraminifera were found in all samples from 0–1 cm and 1–2 cm intervals, while again no living foraminifera were observed in the 2–3 cm interval (**Figure 4** and **Table 2**). Rose Bengal stained aliquots indicated presence of foraminifera (live + recently dead) in cores MC893A, MC893B, MC884, MC880A, and MC880B in all sampling intervals. No Rose Bengal stained individuals were observed in the 1–2 cm and 2–3 cm samples at site MC886 (**Figure 4** and **Table 3**). Both the chi-square (p = 1, α = 0.05) and Student's t-test (p = 0.44, α = 0.05) test show significant differences between number of fluorescently labeled and Rose Bengal stained specimens, within any given sediment interval. In general, there was a lower number of foraminifera in the cold-seep samples than in the control samples. Density of fluorescently labeled foraminifera at Vestnesa Ridge ranged from 0 to 11.1 individuals per 10 m^3 in the 0–1 cm intervals, and from zero to five individuals per 10 cm^3 in the 1–2 cm intervals. Density of live foraminifera at control sites ranged from 7.7 to 14.2 individuals per 10 cm^3 in the 0–1 cm intervals, and from 1.5 to 6.1 in the 1–2 cm intervals (**Figure 4**). The number of Rose Bengal stained

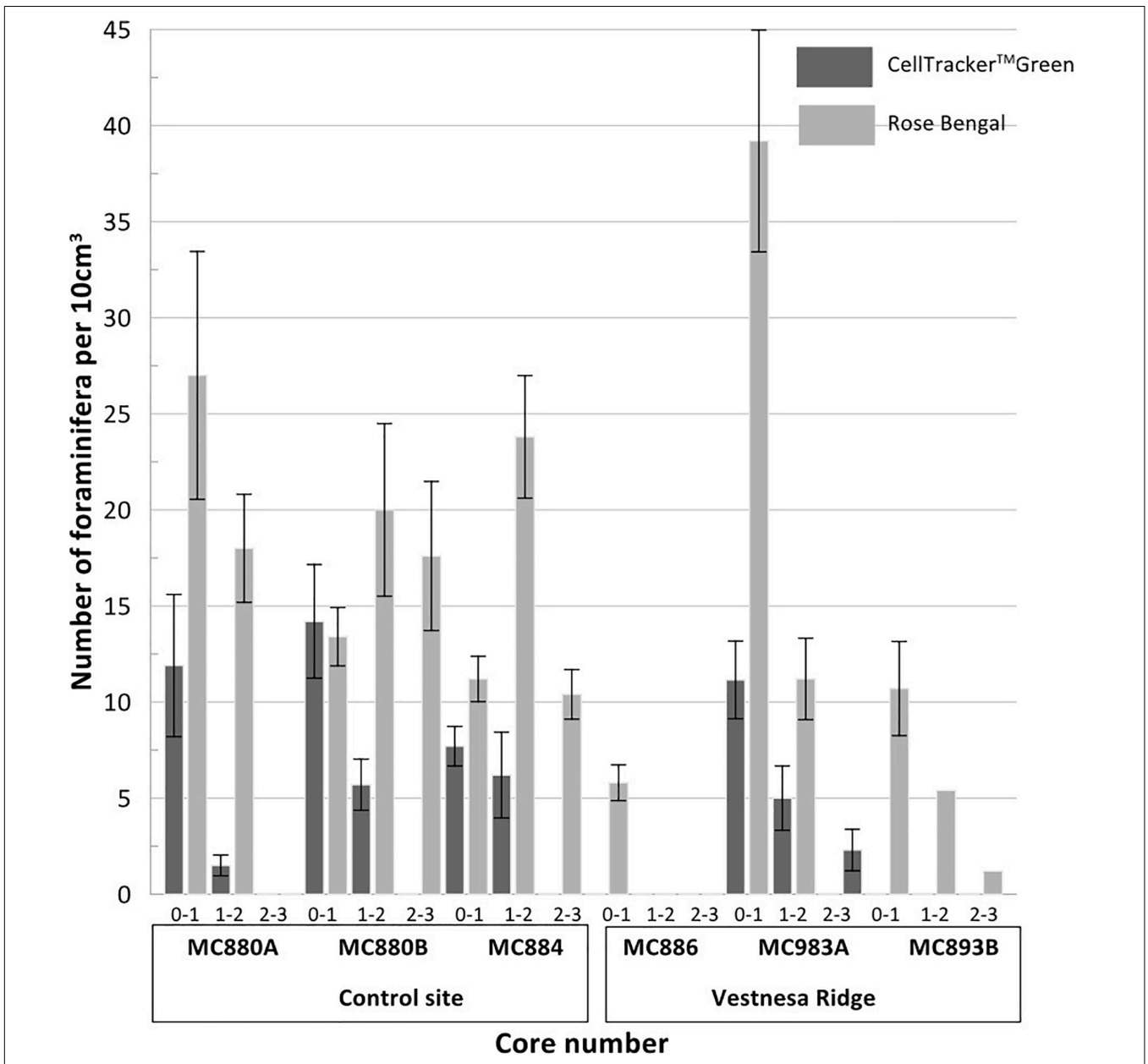

FIGURE 4 | Plots presenting the number (per 10 cm^3) of CellTracker™ Green CMFDA labeled (live) and Rose Bengal stained (live + recently dead) foraminifera from aliquots of Vestnesa Ridge and the nearby control site. Numbers 0–1, 1–2, and 2–3 next to the core number refer to the depth: 0–1, 1–2, and 2-3 cm respectively.

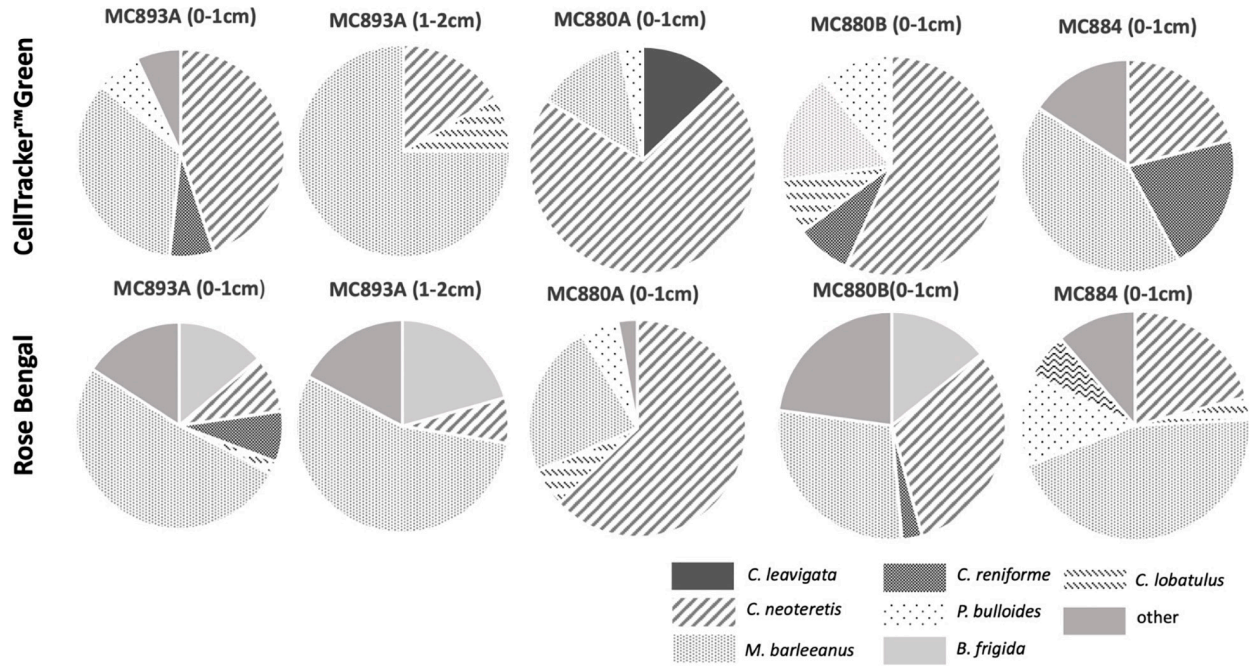

FIGURE 5 | Foraminiferal species composition at Lomvi pockmark (Vestnesa Ridge) and control site using CellTracker^{TM}Green (live) and Rose Bengal (live + recently dead). Plots are based on direct counts (**Tables 2**, **3**).

foraminifera in samples from Vestnesa Ridge active sites ranged from 5.8 to 39.2 individuals per 10 cm^3 in the 0–1 cm interval, from 0 to 11.2 in the 1–2 cm interval, and from 0 to 2.3 in the 2–3 cm interval (**Figure 4**). In the sediment from the control site, the abundance of Rose Bengal stained (live + recently dead) foraminifera ranged from 11.3 to 27 specimens per 10 cm^3 in the 0–1 cm interval, from 20 to 46 foraminifera in the 1–2 cm interval and from 0 to 17.2 in the 2–3 cm interval (**Figure 4**).

CTG and Rose Bengal show that dominant and most common species were the same in the assemblages from active seep sites at Vestnesa Ridge (**Tables 2**, **3** and **Figure 5**). The S(H) index in CTG labeled samples from Vestnesa Ridge range from 0 (empty samples) to 1.33, and from 0.56 to 1.41 in samples from the control site. The S(H) index in Rose Bengal stained samples from Vestnesa Ridge range from 0 (empty sample) to 1.33, and from 1.04 to 1.8 in control site. The Pielou evenness index in CTG labeled samples from Vestnesa Ridge range from 0.58 to 0.88 and from 0.60 to 0.87 in samples from the control site (**Table 2**). In Rose Bengal stained samples the same index varies from 0.44 to 0.78 for Vestnesa Ridge and from 0.48 to 0.76 for the control site (**Table 3**).

In the fluorescently labeled samples from Vestnesa Ridge the foraminiferal faunas are dominated by *M. barleeanus* (34% of total fauna in the 0–1 cm interval and 69% in the 1–2 cm interval) and *C. neoteretis* (45% of total fauna in the 0–1 cm interval and 15% in the 1–2 cm interval) (**Table 2**). Similarly, in Rose Bengal-stained samples the most abundant species were *M. barleeanus* (51% of total fauna in the 0–1 cm interval and 55% in the 1–2 cm interval), *C. neoteretis* (9% of total fauna in the 0–1 cm interval and 7% in the 1–2 cm interval) and *Buccella frigida* (14% of the total fauna in the 0–1 cm interval and 6% in the 1–2 cm interval) (**Table 3**). No apparent endemic foraminiferal species were observed in the Vestnesa Ridge seep sediment samples (**Tables 2**, **3**).

Storfjordrenna Pingos

Metabolically active (fluorescently labeled) benthic foraminifera were present in both the active GHP1 and the inactive GHP5, except at site MC902 taken at the top of the active GHP1 (**Table 4**). In addition to live, metabolically active foraminifera, Rose Bengal staining shows presence of recently dead individuals, i.e., foraminiferal tests that still contain cytoplasm, but were not metabolically active at the time of collection, which could lead to a significant overestimation of the number of live foraminifera ($p = 0.01$, $\alpha = 0.05$; chi-square test) (**Figure 7**).

The ratio between fluorescently labeled and Rose Bengal-stained foraminifera differed between the active and inactive GHP1 and GHP5. A higher proportion of live to recently dead individuals was found in the inactive GHP5, and in GHP1 (except for the sample MC902, which appeared to be barren; **Figure 7**). The ratio between live vs. recently dead foraminifera was approximately 2:3 in the active GHP1, and 3:2 in the inactive GHP5 (**Figure 7**).

At GHP1, the density of live individuals increased along the transect from 0 individuals at the top of GHP1 to 11.84 (per 10 cm^3) at the edge of the pingo. At GHP5 (the non-active site), the foraminifera were relatively evenly distributed compared to the active GHP1. Similarly, to GHP1, the lowest density 3.43 (per 10 cm^3) of metabolically active foraminifera was observed in the sediment from the summit of GHP5 (**Table 4**). The S(H) index

TABLE 4 | Number per sample of CellHunt Green labeled (CHG) and Rose Bengal stained (RB) foraminifera (direct count), and Shannon diversity index from active GHP1 and inactive GHP5.

	MC902		MC917		MC919		MC920		MC921		MC922	
	CHG	RB	CHG	RB	CHG	RB	CHG	RB	CHG	RB	CHG	RB
Buccella frigida			4		6	14	2		2		3	
Cassidulina laevigata			2	1			1	1			1	
Cassidulina neoteretis					2	37		5		5		9
Cassidulina reniforme				4	1	6						3
Cibicides lobatulus			3	14	1	4	1	13	1	10		
Elphidium excavatum			1		8				3		8	
Globobulimina turgida				2	1	4	4	5	2	1	1	2
Melonis barleeanus			8	8	22	31	9	12	30	22	24	2
Nonionellina labradorica			6	3	18	18	10	5		1	3	
Pullenia bulloides				2		5		1	1	3	2	3
Stainforthia loeblichi						1						
Triloculina sp.				1								1
Uvigerina sp.				1	3	2		1				
Total number/sample			24	36	62	122	27	43	39	42	42	20
#Taxa			6	9	9	10	6	8	6	6	7	6
Shannon index			1.53		1.75		1.3		1.08		1.26	
Evenness index			0.83	0.65	0.59	0.63	0.71	0.70	0.40	0.61	0.54	0.77
Chao1 index			6	10	10.5	10	6.5	11	6.3	7	7.5	6

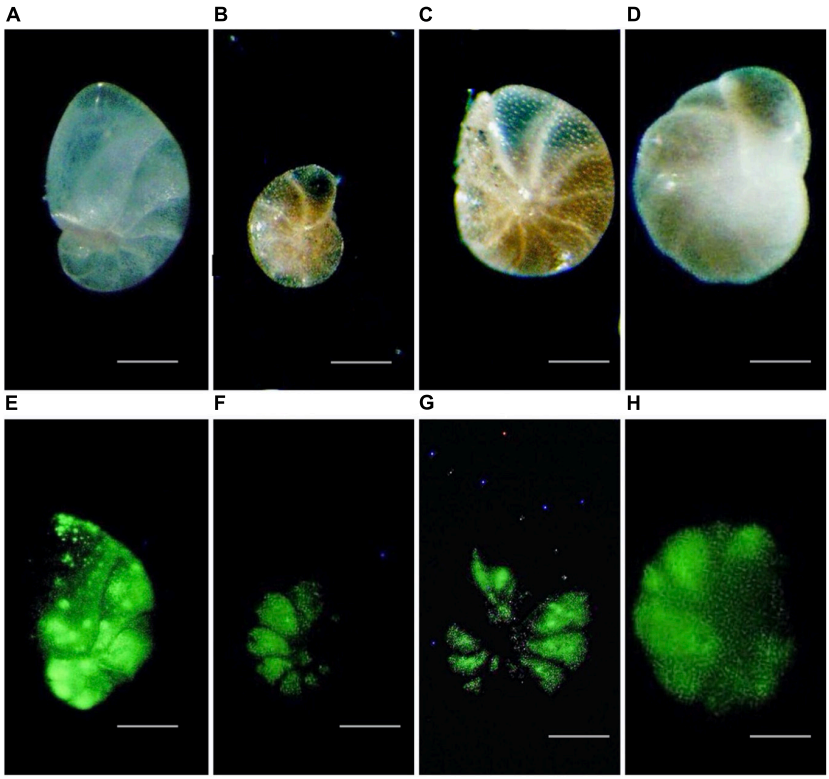

FIGURE 6 | Reflected light **(A–D)** and corresponding epifluorescence (green coloration from CellTracker™ Green) **(E–H)** micrographs of foraminifera collected at Vestnesa Ridge (core 893A); **(A,E)** *Nonionellina labradorica*; **(B,C,G,F)** *Melonis barleeanus*; **(D,H)** *Cassidulina neoteretis*. Scales: panels **(A–D)** = 30 μm; panels **(B,C,F,G)** = 25 μm.

in samples from GHP1 ranged from 0 closer to the center to 1.75 at the edge, and in GHP5 from 1.08 to 1.26 (**Table 4**). The Pielou evenness index in CHG labeled samples from GHP1 varies from 0.59 to 0.83 and between 0.40 and 0.71 in GHP5 (**Table 4**).

Both the active and the post-active pingo were characterized by presence of the same dominant CHG labeled species: *M. barleeanus* (35% of total living fauna in GHP1, and 52% in GHP5), *N. labradorica* (28% in GHP1, and 11% in GHP5), *Elphidium excavatum* (11% in GHP1, and 9% in GHP5) and, to some extent, *B. frigida* (12% in GHP1; **Figure 8**). In the Rose Bengal-stained (i.e., recently dead) samples, the dominant species were *M. barleeanus* (25% of the total living fauna in GHP1, and 34% in GHP5), *C. neoteretis* (23% in GHP1, and 18% in GHP5), *C. lobatulus* (22% in GHP5), and to some extent *N. labradorica* (13% in GHP1, and 6% in GHP5) (**Figure 8**). No endemic species were found in any of the samples from GHP1 or GHP5 (**Figure 8**).

Isotopic Signatures

CellTracker™ Green labeled foraminifera tend to have less negative $\delta^{13}C$ signatures compared to Rose Bengal stained pools and empty tests of their conspecifics, both at Vestnesa Ridge (core MC893A) and at the control site (core MC880A and MC880B; **Figure 9**). The difference between $\delta^{13}C$ measured in CTG labeled individuals and Rose Bengal-stained specimens is 0.22‰ in samples from Vestnesa Ridge, whereas in samples from the control site the difference is 0.41 and 0.15‰. The difference between $\delta^{13}C$ measured in CTG labeled and empty tests is 0.29 and 0.22‰ at Vestnesa Ridge, and between 0.04 and 0.27‰ at the control site (**Table 5**).

In contrast, in both GHP1 and GHP5 the $\delta^{13}C$ values measured in CHG labeled pools are always considerably more depleted compared to values measured in Rose Bengal-stained specimens (**Figure 8**). The difference in $\delta^{13}C$ values in CHG labeled foraminifera is 0.08‰ (at GHP1) and 0.20 and 0.49‰ (at GHP5; **Table 5**). The difference between $\delta^{13}C$ values measured in CHG labeled foraminifera and unstained tests is 0.88 and 1.46‰ at GHP1 and range between 0.14 and 0.58‰ at GHP5. The most pronounced difference is found in samples from the active GHP1 (MC919), where the isotopic signature of live *M. barleeanus* is more depleted compared to the signature of dead individuals (about 1.46‰; **Table 5** and **Figure 8**).

DISCUSSION

Foraminiferal Fauna

The study shows presence of living foraminifera in sediments from active methane emission sites from pockmarks at Vestnesa Ridge and from hydrate mounds ("pingos") in Storfjordrenna.

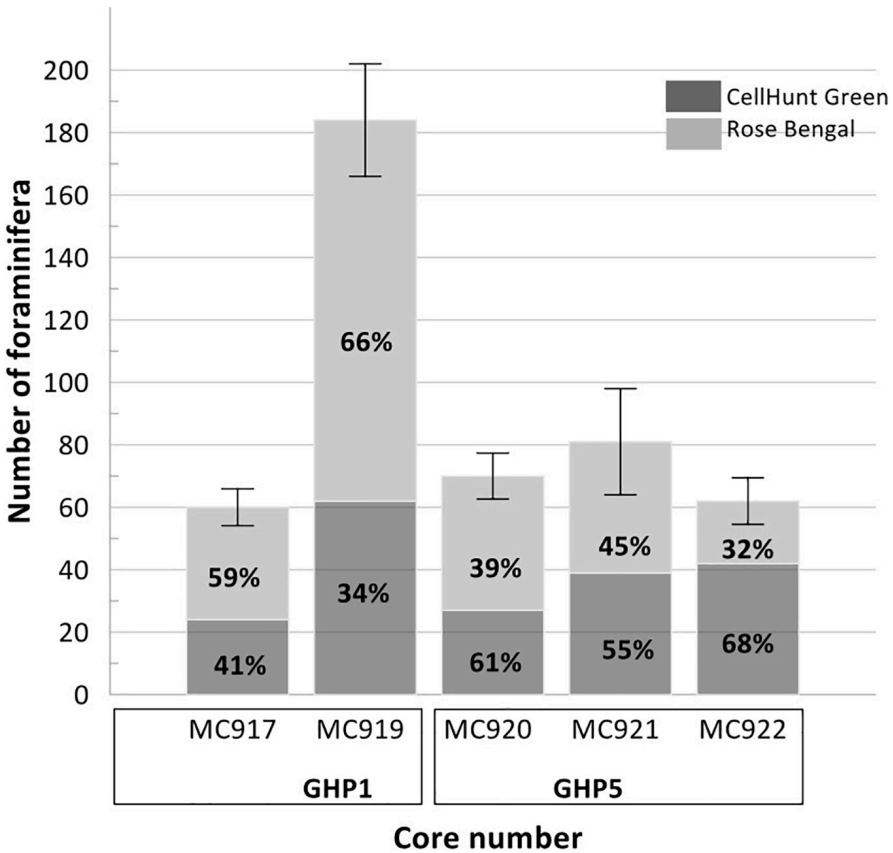

FIGURE 7 | Percentages of benthic foraminifera labeled with CellHunt Green (CHG) = live, and individuals subsequently stained with Rose Bengal (RB) = recently dead (direct count) from Storfjordrenna pingo. The number of foraminifera represents the sum of CHG (dark gray) and RB (light gray) individuals. Plot based on direct counts.

Results imply that, despite the hostile conditions (e.g., low oxygen, high carbon dioxide concentrations and potentially also hydrogen sulfide), which are a result of anaerobic methane oxidation (Herguera et al., 2014), the benthic foraminifera were metabolically active. Furthermore, the results confirmed a previous observation that Rose Bengal staining overestimated the number of live foraminifera (Bernhard et al., 2006). This is manifested for example by the presence of Rose Bengal stained foraminifera in samples with no fluorescently labeled individuals, or by a higher number of Rose Bengal stained foraminifera compared to fluorescently labeled individuals (see samples MC917 and MC919 from Storfjordrenna; **Figure 7**).

Considering the sampling location and previously published studies from Vestnesa Ridge (e.g., Panieri et al., 2017; Sztybor and Rasmussen, 2017; Åström et al., 2018; Dessandier et al., 2019, 2020; Yao et al., 2019), the uneven distribution of foraminifera is most likely a result of the horizontal distribution of geochemically diverse microhabitats within the Vestnesa sediments. The TowCam imaging survey during the sampling campaign revealed a patchy distribution of organisms, such as white and gray bacterial mats and tubeworms (**Figure 2**), which correspond to geochemically different microhabitats (e.g., Niemann et al., 2006; Treude et al., 2007). For example, gray bacterial mats (*Arcobacter* spp., *Thiomargarita* spp.) are common in unstable environments, whereas white bacterial mats (*Beggiatoa* spp.) and tubeworms fields indicate stable sulfide conditions (e.g., Sahling et al., 2002; Niemann et al., 2006; Treude et al., 2007). It has been previously observed that in response to a heterogeneous distribution of methane-dependent microbial and macrofaunal biota, the foraminiferal species composition and absolute abundance (density) may show great variability within the same seep area (e.g., Rathburn et al., 2000; Wollenburg and Mackensen, 2009; Dessandier et al., 2019).

In this study, CTG shows the lowest number or absence of metabolically active foraminifera in some of the assemblages from Vestnesa Ridge, which indeed can be interpreted as an environment being inhospitable for foraminifera. At the same time, in the samples from the MC886 site with no fluorescently labeled individuals, Rose Bengal stained foraminifera (mostly agglutinated taxa) are still present. This observation suggests that "inhospitable" conditions are temporary variations rather than permanent constraints. Instability/variability of the environment can be related to the ephemeral nature of methane seeps, which are strongly dependent on methane

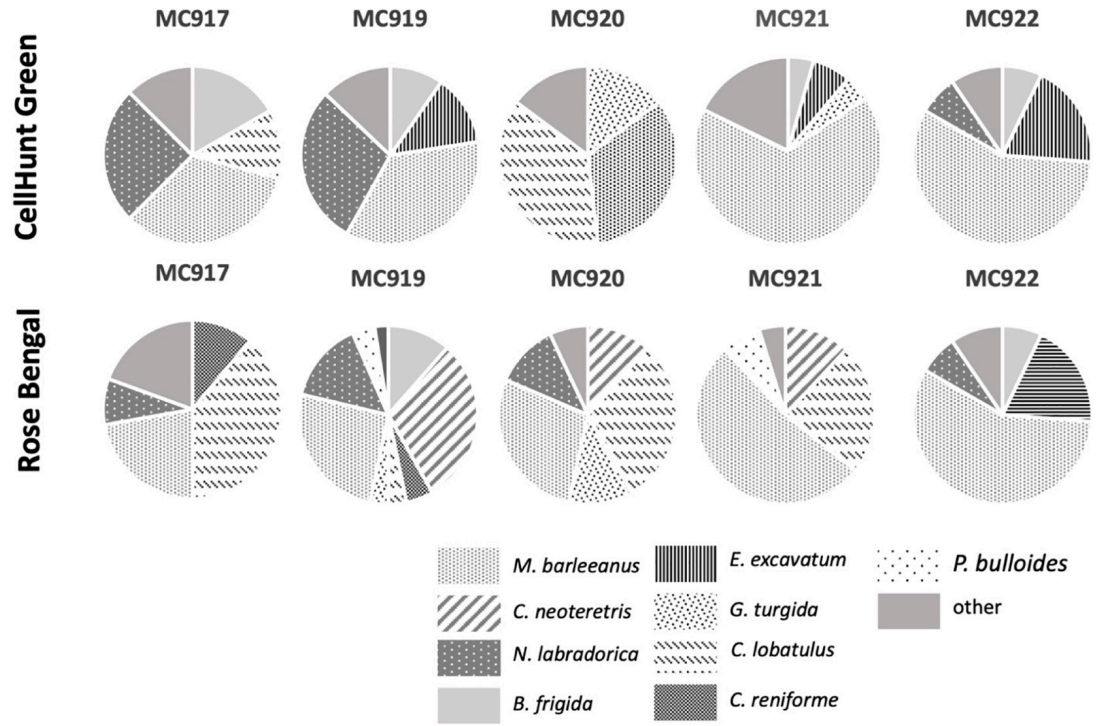

FIGURE 8 | Foraminiferal species composition within the active GHP1 (MC917 and MC919) and post- active GHP5 (MC920, MC921, and MC922). CellHunt Green labeled samples **(upper panel)** and Rose Bengal stained **(lower panel)**.

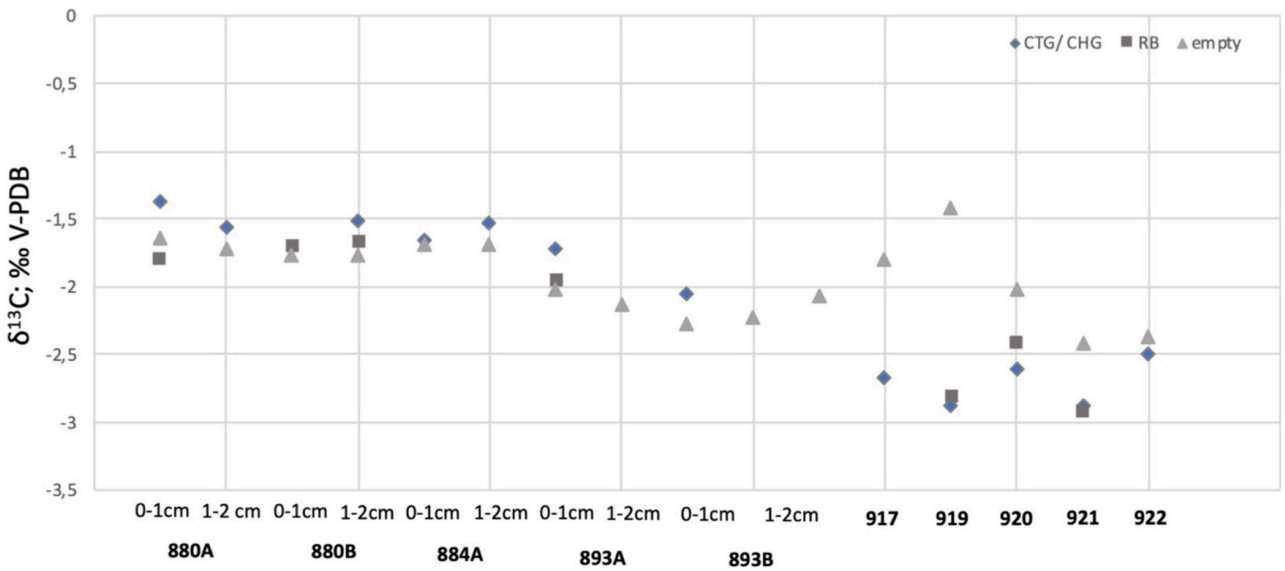

FIGURE 9 | The $\delta^{13}C$ values measured in CellTracker™ Green labeled (CTG), CellHunt Green labeled (CHG), Rose Bengal stained (RB), and empty tests of *Melonis barleeanus*.

flux (Levin, 2005; Åström et al., 2020). As shown by Yao et al. (2019), the Lomvi (MC893) and Lunde (MC886) pockmarks are characterized by two different types of methane transport: advective and dominated by methane diffusion (Lomvi and Lunde, respectively). Additionally, sulfate and methane profiles within the MC886 core indicate non-steady-state conditions (Yao et al., 2019). Those unstable conditions could explain the lack of metabolically active foraminifera with a presence

of Rose Bengal stained specimens in the samples from Lunde pockmark (MC886) at the time of sampling. Similar observations were made by Dessandier et al. (2019): the authors suggested a correlation between low density of foraminifera and methane-diffusive areas due to high sulfide concentration, and decreased or lack of agglutinated foraminifera in cold seep assamblagdes as a result of an increase in organic matter content due to methane related microbial mass, and stronger competition from calcareous species.

Similarly to Vestnesa Ridge, the benthic foraminiferal distribution pattern within the active GHP1 shows a greater variability along the analyzed transect compared to the transect along the inactive GHP5. The highest density of foraminifera is observed at the edge of GHP1, where white and gray bacterial mats are present, with a small difference in density toward the center of GHP1, and reaching zero individuals approximately at the top, where most of the methane flares are located (Serov et al., 2017; Carrier et al., 2020). The $\delta^{13}C_{DIC}$ value at the top of the active GHP reached −24.2‰, which can be linked to methane-related microbial activity (Dessandier et al., 2019). The absence of foraminifera at the summit is thus most likely due to the combined effect of disturbance caused by gas bubbles passing though the sediment and geochemical constraints related to microbial activity (e.g., low oxygen or presence of hydrogen sulfide; Herguera et al., 2014; Carrier et al., 2020). The Shannon index shows that the suite of samples from GHP 5 has less variability compared to the samples from GHP1. The highest density and diversity are observed at the edge of GHP1 (MC919), in bacterial mats. Similarly to other methane cold seeps, the microbial community at the active GHP1 might serve as a food source and support benthic foraminiferal growth (e.g., Rathburn et al., 2000; Panieri, 2006; Fontanier et al., 2014; Herguera et al., 2014).

It is widely accepted that the distribution of benthic foraminiferal faunas at cold seeps is mainly controlled by oxygen levels and organic content, and that species preferring organic-rich environments and reduced oxygen are well adapted to live in the environmental conditions of seep sites (e.g., Akimoto et al., 1994; Rathburn et al., 2000, 2003; Bernhard et al., 2001; Fontanier et al., 2014). In fact, the living foraminiferal fauna at Vestnesa Ridge is dominated by *M. barleeanus* and *C. neoteretis,* and by *M. barleeanus* and *N. labradorica* at the active GHP1. *M. barleeanus* is described as an intermediate to deep infaunal species associated with high-nutrient conditions and resistant to environmental stress due to organic matter degradation (e.g., Wollenburg and Mackensen, 1998; Alve et al., 2016). Both *M. barleeanus* and *C. neoteretis* have been previously observed as the most abundant species in methane-charged sediments at Vestnesa Ridge (Dessandier et al., 2019). Additionally, the TEM (transmission electron microscopy) analyses of *M. barleeanus* from Lomvi pockmark (MC893) at Vestnesa Ridge revealed presence of methanotrophic-like bacteria located outside the test, but very close to their apertural region (Bernhard and Panieri, 2018). Although a possible symbiosis between *M. barleeanus* and methanotrophs remains unconfirmed, the potential influence of seep-related bacteria on *M. barleeanus* cannot be excluded. Similarly, to *M. barleeanus, C. neoteretis* (Rose Bengal stained) was found to be dominant in the top layers of the dysoxic (low oxygen) sediments of the Håkon Mosby Mud Volcano (Wollenburg and Mackensen, 2009) and was one of the most numerous species at Vestnesa Ridge (Dessandier et al., 2019). As in other investigated methane seep sites, to date, there are no endemic species found at Vestnesa Ridge and Storfjordrenna pingos, but only well-known species represented in a wide range of environments (e.g., Rathburn et al., 2000; Bernhard et al., 2001; Herguera et al., 2014; Dessandier et al., 2019).

The combined use of CHG and Rose Bengal allows to distinguish live and recently dead foraminifera from the Storfjordrenna area, which reveals major shifts in species compositions in both the active GHP1 and the inactive GHP5. In live foraminiferal assemblages, the most common species after *M. barleeanus* are *N. labradorica* and *E. excavatum,* whereas in Rose Bengal stained samples *C. neoteretis* and *C. lobatulus* are of high relative abundance. Because species which tolerate high organic concentration and low oxygen conditions are associated both with spring bloom and methane seepage, it is challenging to distinguish precisely to what extent the switch in population is due to methane availability. Particularly, the relatively high number of live *N. labradorica* both in the active GHP1 and inactive GHP5, as well as appearance of *E. excavatum*, might indicate the influence of the seasonal algae bloom. *E. excavatum* is an opportunistic species, with the ability to respond rapidly to deposition of food (pulsed food supply; Corliss, 1991; Altenbach, 1992) and colonize harsh environments (Korsun and Hald, 2000). It almost completely replaces other species, such as *C. lobatulus*, which is an epifaunal species that prefers low food supply and high oxygen concentration (e.g., Hald and Steinsund, 1996; Klitgaard-Kristensen et al., 2002). The significant number of *N. labradorica* and *B. frigida* in samples MC919 from GHP1 is puzzling. Although *N. labradorica* is known to feed on fresh phytodetritus, and is an indicator species of high primary productivity as a result of the retreating summer sea-ice margin or Arctic Front (Cedhagen, 1991; Corliss, 1991), this species also has a potential to thrive at methane seepage sites. *N. labradorica* (Rose Bengal stained) have been found previously in the sediment from the top of the GHP1 (Dessandier et al., 2020). Kleptoplasts present in cell of *N. labradorica* might be involved in ammonium or sulfate assimilation pathways and might potentially support life under adverse conditions (Jauffrais et al., 2019). Alike *N. labradorica,* the distribution of *B. frigida* is related to seasonal sea-ice retreat and appearance of fresh algae (Seidenkrantz, 2013). From all investigated samples from Storfjordrenna, *B. frigida* occurs most frequently in the MC919 samples, where bacterial mats are present. In previous studies from Vestnesa Ridge, it was suggested that the species potentially can feed on microbial food sources, i.e., methane related bacterial mats (Dessandier et al., 2019). Interestingly, in this study *B. frigida* occur in CTG labeled samples, but there were no Rose Bengal stained individuals. This suggests that presence of live *B. frigida* might reflect a relatively recent appearance of bacterial mats associated with methane seepage.

Additionally, the use of both CHG and Rose Bengal reveals a difference in the percentage of living vs. recently dead

TABLE 5 | Carbon isotope values ($\delta^{13}C$; ‰ V-PDB) of *Melonis barleeanus*, *Cassidulina neoteretis*, and *Neogloboquadrina pachyderma*, and dissolved inorganic carbon (DIC; *Bernhard and Panieri, 2018) from Vestnesa Ridge and control site; and *Melonis barleeanus* and *Nonionellina labradorica* from Storfjordrenna pingo from active GHP1 and inactive GHP5; CellTracker™ Green CMFDA (CTG), CellHunt Green (CHG), Rose Bengal (RB) individuals, and empty tests.

			M. barleeanus			*C. neoteretis*			*N. pachyderma*	*N. labradorica*			DIC*
	Core number	**Depth (cm)**	**CTG/CHG δ ^{13}C**	**RB δ ^{13}C**	**Empty δ ^{13}C**	**CTG δ ^{13}C**	**RB δ ^{13}C**	**Empty δ ^{13}C**	**Empty δ ^{13}C**	**CHG δ ^{13}C**	**RB δ ^{13}C**	**Empty δ ^{13}C**	**δ ^{13}C**
Vestnesa Ridge	MC893A	0–1	−1.73	−1.95	−2.02	−0.26			−0.63				
					−2.14				−0.22				
		1–2	−2.06		−2.28			−0.66					
	MC893B	0–1			−2.24								−3.34
		1–2			−2.08								−14.25
Control site	MC880A	0–1	−1.38	−1.79	−1.65				−0.33				
		1–2	−1.57		−1.72								−0.79
	MC880B	0–1		−1.70	−1.77	−0.38							
		1–2	−1.52	−1.67	−1.78	−0.35							−0.64
	MC884	0–1	−1.66		−1.70				−0.84				
		1–2	−1.54		−1.70								
GHP 1	MC917	0–1	−2.68		−1.80								
	MC919	0–1	−2.89	−2.81	−1.43					−4.34	−4.34		
GHP5	MC920	0–1	−2.61	−2.41	−2.03					−4.21	−3.38		
	MC921	0–1	−2.89	−2.92	−2.43					−3.38			
	MC922	0–1	−2.51		−2.37								

foraminifera within each of the investigated GHP types. The active GHP1 is characterized by a greater percentage of recently dead (Rose Bengal stained) individuals, compared to living (CHG labeled) specimens, whereas in the inactive GHP5 pingo this ratio is reversed with more live than dead foraminifera. This difference between the active GHP1 and inactive GHP5 implies more unstable and variable environmental conditions at GHP1, potentially related to methane emissions, rather than general seasonal environmental changes (Carrier et al., 2020). On average, CHG labeling showed that approximately 40% of the benthic foraminifera in GHP1 and approximately 54% in GHP5 were alive at the time of collection.

Interestingly, despite the highest number of living foraminifera in GHP5 the Pielou evenness index in CHG labeled samples shows fairly low values (from 0.40 to 0.71) compared to samples from GHP1 (from 0.59 to 0.83) (**Table 4**). It indicates the presence of dominant, well-adapted species in the foraminiferal population within the post-active GHP, most likely due to the recent environmental changes. Because, the Pielou evenness index is relatively low in the post-active GHP5 compared to GHP1, we can exclude methane influence. It is possible the evenness index decreased due to the influence of the spring bloom. In the literature methane cold seeps are described as a biological oasis in the high−Arctic deep sea (Åström et al., 2018) due to the presence of microbial communities seeps provide enough food to sustain foraminiferal populations (e.g., Rathburn et al., 2000; Torres et al., 2003; Heinz et al., 2005; Panieri, 2006; Panieri and Sen Gupta,2008). In contrast, sediments outside the seeps are impoverished in organic substrates for most of the year and depend on benthic-pelagic coupling (Gooday, 1988). Thus, the benthic communities in the Arctic, which experience low food are likely more sensitive to food input from primary production (e.g., Gooday, 1988, 1993; Sander and van der Zwaan, 2004; Nomaki et al., 2005; Schönfeld and Numberger, 2007; Braeckman et al., 2018). After the episode of strong food pulses, a population of specific opportunistic species increased, which can quickly utilize large amounts of detritus (e.g., Gooday, 1988; Nomaki et al., 2005; Braeckman et al., 2018). In fact, samples from GHP5 are dominated by *M. barleeanus*, an opportunistic species well adapted to high organic content (e.g., Wollenburg and Mackensen, 1998; Alve et al., 2016) and shows a relatively high number of *E. excavatum*. A " bloom-feeding" behavior of *E. excavatum* was previously described by Schönfeld and Numberger (2007). In comparison, the foraminiferal fauna from the active GHP consists mainly of species such as *B. frigida* and *N. labradorica*, species that thrive in cold seeps and can feed on bacteria (e.g., Dessandier et al., 2019; Jauffrais et al., 2019).

The $\delta^{13}C$ Signature in Foraminiferal Tests

Within methane cold seeps, the geochemistry of pore water is influenced by aerobic and/or anaerobic methane oxidation (Treude et al., 2007). Because methane-derived carbon is characterized by very low carbon isotopic signatures (from −50 to −20‰ for thermogenic methane, and from −110‰ to −60‰ for microbial methane) (Whiticar, 1999), the ambient DIC pool is enriched in isotopically light carbon in the form of either carbon dioxide (CO_2) or bicarbonate (HCO_3^-) resulting from microbial activity. If foraminifera incorporate methane-derived carbon from the ambient seawater during biomineralization, we would expect to see more negative $\delta^{13}C$ values in their tests compared to $\delta^{13}C$ values in tests of foraminifera from the non-seep sites. At Lomvi pockmark (Vestnesa Ridge), the $\delta^{13}C$ measured on CTG labeled, Rose Bengal stained, and unstained tests of *M. barleeanus* have values within the same range as of its conspecifics in "normal" (non-seep) marine environments, i.e., approximately −2‰ (e.g., Wollenburg et al., 2001; Dessandier et al., 2020). Likewise, the $\delta^{13}C$ measured on live *C. neoteretis* showed values within the expected range for specimens from non-seep environments, i.e., approximately −0.3‰ to −1‰ (Wollenburg et al., 2001), and was not as depleted as previously reported values (−7.5‰ $\delta^{13}C$) measured on Rose Bengal stained *C. neoteretis* from Håkon Mosby Mud Volcano (Mackensen et al., 2006). Therefore, the data provide no clear evidence that *M. barleeanus* and *C. neoteretis* from Vestnesa Ridge incorporate significant amounts of methane-derived carbon during test formation that would markedly affect the isotopic signature of their carbonate tests. The difference between $\delta^{13}C$ signatures of *M. barleeanus* and *C. neoteretis* most likely reflects different microhabitat preferences of these species. Infaunal species, such as *M. barleeanus,* tend to have more negative $\delta^{13}C$ compared to, for example, epifaunal or shallow infaunal species, such as *C. neoteretis* (e.g., Grossman, 1984; McCorkle et al., 1985; Fontanier et al., 2006).

The $\delta^{13}C$ measured in both metabolically active (CHG labeled) and recently dead (Rose Bengal stained) foraminifera from Storfjordrenna pingos is not straightforward to interpret. Although the $\delta^{13}C$ in tests of fluorescently labeled foraminifera from the active GHP1 have values slightly more depleted than the values exhibited by the same species in the post-active GHP5, still the $\delta^{13}C$ values measure in *M. barleeanus* from both GHPs are not much more depleted compared to Rose Bengal stained conspecific from near non-seep site (i.e., lower than −2.1‰; Dessandier et al., 2019). Overall, the $\delta^{13}C$ measured in *M. barleeanus* from Storfjordrenna are not significantly depleted compared to isotopic signatures of other seep-site foraminifera, e.g., *Uvigerina peregrina* with measured $\delta^{13}C$ values down to −5.64‰ (Hill et al., 2004), or *C. neoteretis* with $\delta^{13}C$ values of −7.5‰ (Mackensen et al., 2006). Storfjordrenna is at a relatively shallow water depth (∼400 m) and the sediment samples were collected in June. Thus, the negative $\delta^{13}C$ signature in foraminiferal tests could originate from a greater flux of particulate organic matter produced during the spring bloom and only potentially partly from methane seepage. A shift of approximately 0–4‰ toward a more negative $\delta^{13}C$ is shown to have an origin in local organic matter degradation (e.g., Torres et al., 2003; Martin et al., 2004).

It is generally believed that more negative $\delta^{13}C$ signatures in unstained and/or fossil foraminifera compared to those of "living" (Rose Bengal stained) specimens result from an authigenic overgrowth layer covering the tests. Foraminiferal tests deposited in methane-charged sediments might be coated by precipitates from highly ^{13}C-depleted pore water or

bacterially mediated methane oxidation and associated carbonate precipitation (e.g., Rathburn et al., 2003; Torres et al., 2003; Schneider et al., 2017; Sztybor and Rasmussen, 2017). A similar interpretation can be applied to explain the offset in $\delta^{13}C$ values between Rose Bengal stained and fluorescently labeled *M. barleeanus* from Vestnesa Ridge. Since Rose Bengal stained foraminifera represent both live and recently dead individuals, it is possible that in some of the specimens the organic lining was already partially decomposed, and that this surface of the tests had authigenic carbonate overgrowths (Mackensen et al., 2006). Considering the fact that isotopic offset occurred both in samples from Lomvi and the control site, and the isotopic variation is relatively low (∼0.20‰ Vestnesa Ridge, 0.15 and 0.41‰ at the control site), the offset could be due to dissolution of biogenic calcite and re-precipitation of inorganic calcite (overgrowth and recrystallization) or other early diagenetic processes that occur in normal non-seep sediments (Ravelo and Hillaire-Marcel, 2007), and as such not necessarily the effect of Methane-Derived Authigenic Carbonates (MDAC) overgrowth. Additionally, $\delta^{13}C$ values recorded in unstained tests of the planktonic foraminifera *N. pachyderma* from Vestnesa Ridge are close to the expected $\delta^{13}C$ values for normal "Holocene" marine environments (−0.5 to 0.5‰; Zamelczyk et al., 2014; Werner et al., 2016). Because planktic foraminifera live and calcify in the water column, significantly depleted $\delta^{13}C$ signature (−7‰ or higher; Torres et al., 2003) in their unstained tests results from diagenetic overgrowth by authigenic carbonates associated with aerobic methane oxidation (AOM; Torres et al., 2003; Uchida et al., 2004; Martin et al., 2010; Schneider et al., 2017). Values obtained for *N. pachyderma* from Vestnesa Ridge support the inference that benthic foraminiferal assemblages have not been significantly overprinted by MDAC.

Unlike Vestnesa Ridge, in GHP1 and GPH 5 the $\delta^{13}C$ values in the fluorescently labeled *M. barleeanus* are always more negative compared to the $\delta^{13}C$ in Rose Bengal stained and unstained tests. This could suggest that living foraminifera did incorporate methane-derived carbon during biomineralization. Mackensen et al. (2006) suggested that more depleted isotopic $\delta^{13}C$ signatures in living (Rose Bengal stained) foraminifera compared to unstained tests can be interpreted as a result of methane influence. In sample MC919 the difference between $\delta^{13}C$ measured in live *M. barleeanum* compared to value in empty tests is pronounced (about 1.55‰), whereas the difference between $\delta^{13}C$ in live foraminifera and empty tests in the post-active GHP5 does not exceed 0.4‰. Most likely, foraminifera absorbed methane-derived carbon *via* the food web by feeding on methanotrophic bacteria (see section "Foraminiferal Fauna").

Although the $\delta^{13}C$ signatures in tests of live foraminifera from the study areas are not significantly depleted to determine the influence of methane, it should be noted that the $\delta^{13}C$ are measured on pools of specimens (N = ∼10). It is possible that at least some of the individuals had more negative $\delta^{13}C$ signatures than others, or that some chambers indeed incorporated methane-derived carbon, as suggested by Bernhard et al. (2010). However, even if the foraminifera calcified during episodes of high methane flux, it is likely that only parts of the tests were constructed under intense seepage conditions, while the major part of the tests had a pre-seep or post-seep signatures (i.e., carbon isotopes incorporated before or after a seepage event). Methane is only one of the potential carbon sources at cold seeps. In surface sediments, the biological degradation of marine snow contributes to the local DIC pool and might explain the negative signature of the $\delta^{13}C_{DIC}$ (e.g,„ Alldredge and Silver, 1988; Bauer and Druffel, 1998; Torres et al., 2003). As an example, a previous study of the $\delta^{13}C_{TOC}$ values for Vestnesa Ridge showed presence of both classical marine $\delta^{13}C_{TOC}$ and depleted $\delta^{13}C_{TOC}$ related to methane seepage (Dessandier et al., 2019). Thus, if the foraminifera use carbon both from ambient water and intracellular storage (i.e., resulting from respiration and diet; de Nooijer et al., 2009; Toyofuku et al., 2017), it seems unlikely that the isotopic signature of foraminifera only reflects the methane-derived carbon; rather, it may be a result of both non-seep and seep carbon. To obtain more accurate $\delta^{13}C$ values, analysis of single specimens, or more advanced techniques, e.g., secondary-ion mass spectrometry (SIMS) is recommended.

CONCLUSION

1. Labeling with fluorescence probes showed that metabolically active foraminifera were present in methane-influenced sediments both at Vestnesa Ridge and Storfjordrenna. Both sites were characterized by comparable faunal patterns, with no endemic species, and the observed species were similar to those from other non-seep locations within the Arctic Ocean. At Vestnesa Ridge, and at the non-seep control site off Vestnesa Ridge, the most abundant calcareous species were *M. barleeanus* and *C. neoteretis*. In Storfjordrenna in both GHP environments, the foraminiferal faunas were dominated by *M. barleeanus* and *N. labradorica*.
2. Methane seepage did not markedly affect the isotopic signature ($\delta^{13}C$) of primary calcite in metabolically active foraminifera. One exception was sample MC919, where a more negative isotopic signature of *M. barleeanus* could potentially reflect methane influence.
3. The results of this study show the effectiveness of fluorescent probes in ecological studies. At Vestnesa Ridge, Rose Bengal staining overestimated the number of living foraminifera, indicating a higher number of live foraminifera compared to the CTG labeled specimens (23% of foraminifera were live at Vestnesa Ridge and 34% at the control site).
4. The is no significant difference between $\delta^{13}C$ measured in fluorescent labeled foraminifera and Rose Bengal stained.
5. At Storfjordrenna, the combined use of CHG and Rose Bengal allowed to distinguish between living and recently dead benthic foraminifera. This demonstrated a marked change in the foraminiferal population from a *C. neoteretis/Cibicides lobatulus* dominated assemblage to an assemblage dominated by *M. barleeanus* and *N. labradorica,* which otherwise would have been overlooked. Despite the more time-consuming protocol compared to Rose Bengal staining, the fluorescent viability

assays such as CHG and CTG CMFDA have a great advantage and it is advised that they be applied more often in studies of the ecology of benthic foraminifera.

DATA AVAILABILITY STATEMENT

The original contributions presented in the study are included in the article/supplementary material, further inquiries can be directed to the corresponding author/s.

AUTHOR CONTRIBUTIONS

KM collected and processed the samples, analyzed data, and wrote the manuscript.

FUNDING

This work was supported by the Research Council of Norway through its Centers of Excellence funding scheme grant 287 no. 2232.

ACKNOWLEDGMENTS

The author would like to thank the captain and crew of the R/V *Helmer Hansen* and chief scientist G. Panieri during CAGE15-2 cruise and AMGG CAGE17-2 cruise, A.G. Hestnes for support assistance in work with a fluorescence microscope, and A. N. Osiecka for linguistic assistance and J. M. Bernhard for comments that greatly improved the manuscript.

REFERENCES

Akimoto, K., Tanaka, T., Hattori, M., and Hotta, H. (1994). "Recent benthic foraminiferal assemblages from the cold seep communities}a contribution to the methane gas indicator," in *Pacific Neogene Events in Time and Space*, ed. R. Tsuchi (Tokyo: University of Tokyo Press), 11–25.

Alldredge, A. L., and Silver, M. W. (1988). Characteristics, dynamics and significance of marine snow. *Prog. Oceanogr.* 20y, 41–82. doi: 10.1016/0079-6611(88)90053-5

Altenbach, A. V. (1992). Short term processes and patterns in the foraminiferal response to organic flux rates. *Mar. Micropaleontol.* 19, 119–129. doi: 10.1016/0377-8398(92)90024-E

Alve, E., Korsun, S., Schönfeld, J., Dijkstra, N., Golikova, E., Hess, S., et al. (2016). Foram-AMBI: A sensitivity index based on benthic foraminiferal faunas from North-East Atlantic and Arctic fjords, continental shelves and slopes. *Mar. Micropaleontol.* 122, 1–12. doi: 10.1016/j.marmicro.2015.11.001

Amap Assessment (2018). *Arctic Ocean Acidification, Arctic Monitoring and Assessment Programme (AMAP)*. Tromsø: AMAP Assessment.

Archer, D., Buffett, B., and Brovkin, V. (2009). Ocean methane hydrates as a slow tipping point in the global carbon cycle. *Proc. Natl. Acad. Sci. U S A.* 106, 20596–20601. doi: 10.1073/pnas.0800885105

Arrigo, K. R., and van Dijken, G. L. (2011). Continued increases in Arctic Ocean primary production. *Prog. Oceanogr.* 136, 60–70. doi: 10.1016/j.pocean.2015.05.002

Åström, E. K. L., Carroll, M. L., Ambrose, W. G. Jr., Sen, A., Silyakova, A., and Carroll, J. (2018). Methane cold seeps as biological oases in the high-Arctic deep sea. *Limnol. Oceanogr.* 63, 209–231. doi: 10.1002/lno.10732

Åström, E. K. L., Carroll, M. L., Ambrose, W. G., and Carroll, J. (2016). Arctic cold seeps in marine methane hydrate environments: Impacts on shelf macrobenthic community structure offshore Svalbard. *Mar. Ecol. Prog. Ser.* 552, 1–18. doi: 10.3354/meps11773

Åström, E. K. L., Sen, A., Carroll, M. L., and Carroll, J. (2020). Cold Seeps in a Warming Arctic: Insights for Benthic Ecology. *Front. Mar. Sci.* 7:244. doi: 10.3389/fmars.2020.00244

Bauer, J., and Druffel, E. (1998). Ocean margins as a significant source of organic matter to the deep open ocean. *Nature* 392, 482–485.

Bernhard, J. M., and Panieri, G. (2018). Keystone Arctic paleoceanographic proxy association with putative methanotrophic bacteria. *Sci. Rep.* 8:10610. doi: 10.1038/s41598-018-28871-3

Bernhard, J. M., Buck, K. R., and Barry, J. P. (2001). Monterey Bay cold-seep biota: Assemblages, abundance, and ultrastructure of living foraminifera. *Deep Sea Res. Part I Oceanogr. Res. Papers* 48, 2233–2249.

Bernhard, J. M., Martin, J. B., and Rathburn, A. E. (2010). Combined carbonate carbon isotopic and cellular ultrastructural studies of individual benthic foraminifera: 2. Toward an understanding of apparent disequilibrium in hydrocarbon seeps. *Paleoceanography* 25:4206. doi: 10.1029/2009PA001846

Bernhard, J. M., Ostermann, D. R., Williams, D. S., and Blanks, J. K. (2006). Comparison of two methods to identify live benthic foraminifera: A test between Rose Bengal and CellTracker Green with implications for stable isotope paleoreconstructions. *Paleoceanography* 21:4210. doi: 10.1029/2006PA001290

Box, J. E., Colgon, W. T., Christensen, T. R., Schmidt, N. M., Lund, M., and Parmentier, F. W. (2019). Key indicators of Arctic climate change: 1971-2017. *Environ. Res. Lett.* 14:045010.

Braeckman, U., Janssen, F., Lavik, G., Elvert, M., Marchant, H., Buckner, C., et al. (2018). Carbon and nitrogen turnover in the Arctic deep-sea: in situ benthic community response to diatom and coccolithophorid phytodetritus. *Biogeosciences* 15, 6537–6557. doi: 10.5194/bg-15-6537-2018

Bünz, S., Polyanov, S., Vadakkepuliyambatta, S., Consolaro, C., and Mienert, J. (2012). Active gas venting through hydrate-bearing sediments on the Vestnesa Ridge, offshore W-Svalbard. *Mar. Geol.* 332-334, 189–197. doi: 10.1016/j.margeo.2012.09.012

Carrier, V., Svenning, M. M., Gründger, F., Niemann, H., Dessandier, P.-A., Panieri, G., et al. (2020). The Impact of Methane on Microbial Communities at Marine Arctic Gas Hydrate Bearing Sediment. *Front. Microbiol.* 11:1932. doi: 10.3389/fmicb.2020.01932

Cedhagen, T. (1991). Retention of chloroplasts and bathymetric distribution in the sublittoral foraminiferan Nonionellina labradorica. *Ophelia* 33, 17–30.

Cordes, E., Bergquist, D., Predmore, B., Dienes, P., Jones, C., Telesnicki, G., et al. (2006). Alternate unstable states: convergent paths of succession in hydrocarbon-seep tubeworm-associated communities. *J. Exp. Mar. Biol. Ecol.* 339, 159–176. doi: 10.1016/j.jembe.2006.07.017

Corliss, B. H. (1991). Morphology and microhabitat preferences of benthic foraminifera from the northwest Atlantic Ocean. *Mar. Micropaleontol.* 17, 195–236. doi: 10.1016/0377-8398(91)90014-W

de Nooijer, L. J., Langer, G., Nehrke, G., and Bijma, J. (2009). Physiological controls on seawater uptake and calcification in the benthic foraminifer *Ammonia tepida*. *Biogeosciences* 6, 2669–2675. doi: 10.5194/bg-6-2669-2009

Dessandier, P. A., Borrelli, C., Kalenitchenko, D., and Panieri, G. (2019). Benthic Foraminifera in Arctic Methane Hydrate Bearing Sediments. *Front. Mar. Sci.* 6:765. doi: 10.3389/fmars.2019.00765

Dessandier, P., Borrelli, C., Yao, H., Sauer, S., Hong, W. L., and Panieri, G. (2020). Foraminiferal $\delta^{18}O$ reveals gas hydrate dissociation in Arctic and North Atlantic Ocean sediments. *Geo Mar. Lett.* 40, 507–523. doi: 10.1007/s00367-019-00635-6

Dickens, G. R., Castillo, M. M., and Walker, J. C. G. (1997). A blast of gas in the latest Paleocene: Simulating first-order effects of massive dissociation of oceanic methane hydrate. *Geology* 25, 259–262. doi: 10.1130/0091-76131997025<0259:abogit<2.3.co;2

Etiope, G., Panieri, G., Fattorini, D., Regoli, F., Vannoli, F. P., Italiano, F., et al. (2014). A thermogenic hydrocarbon seep in shallow Adriatic Sea (Italy): Gas origin, sediment contamination and benthic foraminifera. *Mar. Petroleum Geol.* 57, 283–293.

Figueira, B., Grenfell, Hugh, Hayward, B., and Alfaro, A. (2012). Comparison of rose bengal and CellTracker^{TM} green staining for identification of live salt-marsh foraminifera. *J. Foraminiferal Res.* 42, 206–215.

Fontanier, C., Duros, P., Toyofuku, T., Oguri, K., Koho, K. A., Buscail, R., et al. (2014). Living (stained) deep-sea foraminifera off hachinohe (NE Japan, western Pa- cific): Environmental interplay in oxygen-depleted ecosystems. *J. Foraminiferal Res.* 44, 281–299.

Fontanier, C., Mackensen, A., Jorissen, F. J., Anschutz, P., Licari, L., and Griveaud, C. (2006). Stable oxygen and carbon isotopes of live benthic foraminifera from the Bay of Biscay: Microhabitat impact and seasonal variability. *Mar. Micropaleontol.* 58, 159–183.

Gooday, A. J. (1988). A response by benthic Foraminifera to the deposition of phytodetritus in the deep-sea. *Nature* 332, 70–73.

Gooday, A. J. (1993). Deep-sea benthic foraminifera species which exploit phytodetritus: Characteristic features and controls on distribution. *Mar. Micropaleontol.* 22, 187–205.

Gooday, A. J. (1994). The biology of deep-sea foraminifera: a review of some advances and their applications. *Paleoceanography* 9, 14–31.

Gooday, A. J. (2003). Benthic foraminifera (Protista) as tools in deep-water palaeoceanography: a review of environmental influences on fau- nal characteristics. *Adv. Mar. Biol.* 46, 1–90.

Grossman, E. L. (1984). Stable isotope fractionation in live benthic foraminifera from the southern California Borderland. *Palaeogeogr. Palaeoclimatol. Palaeoecol.* 47, 301–327. doi: 10.1016/0031-0182(84)90100-7

Grossman, E. L. (1987). Stable isotopes in modern benthic foraminifera: a study of vital effect. *J. Foraminifera Res.* 17, 48–61.

Hald, M., and Steinsund, P. I. (1996). "Benthic foraminifera and carbonate dissolution in surface sediments of the Barents-and Kara Seas," in *Surface sediment composition and sedimentary processes in the central Arctic Ocean and along the Eurasian Continental Margin. Berichte zur Polarforschung*, Vol. 212, eds R. Stein, G. I. Ivanov, M. A. Levitan, and K. Fahl (Bremerhaven: Wegener Inst. Polar Meeresforsch), 285–307.

Heinz, P., Sommer, S., and Pfannkuche, O. (2005). Living benthic foraminifera in sediments influenced by gas hydrates at the Cascadia convergent margin, NE Pacific. *Mar. Ecol. Prog. Ser.* 304, 77–89.

Herguera, J. C., Paull, C. K., Perez, E., Ussler, W., and Peltzer, E. (2014). Limits to the sensitivity of living benthic foraminifera to pore water carbon isotope anomalies in methane vent environments. *Paleoceanography* 29, 273–289. doi: 10.1002/2013PA002457

Hill, T. M., Kennett, J. P., and Valentine, D. L. (2004). Isotopic evidence for the incorporation of methane-derived carbon into foraminifera from modern methane seeps, Hydrate Ridge, Northeast Pacific. *Geochim. Cosmochim. Acta* 68, 4619–4627. doi: 10.1016/j.gca.2004.07.012

Hong, W.-L., Torres, M. E., Carroll, J., Cremiere, A., Panieri, G., Yao, H., et al. (2017). Seepage from an Arctic shallow marine gas hydrate reservoir is insensitive to momentary ocean warming. *Nat. Commun.* 8, 1–14. doi: 10.1038/ncomms15745

Hustoft, S., Bünz, S., Mienert, J., and Chand, S. (2009). Gas hydrate reservoir and active methane-venting province in sediments on <20 Ma young oceanic crust in the Fram Strait, offshore NW-Svalbard. *Earth Planetary Sci. Lett.* 284, 12–24. doi: 10.1016/j.epsl.2009.03.038

IPCC (2007). *Climate Change 2007: The Physical Basis*. New York, NY: Cambridge University Press.

IPCC (2013). "The physical science basis," in *Contribution of Working Group I to the Fifth Assessment Report of the Intergovernmental Panel on Climate Change*, eds T. F. Stocker, D. Qin, G.-K. Plattner, M. Tignor, S. K. Allen, J. Boschung, et al. (Cambridge: Cambridge University Press), 1535.

Jauffrais, T., LeKieffre, C., Schweizer, M., Geslin, E., Metzger, E., Bernhard, J. M., et al. (2019). Kleptoplastidic benthic foraminifera from aphotic habitats: insights into assimilation of inorganic C, N and S studied with sub-cellular resolution. *Environ. Microbiol.* 21, 125–141. doi: 10.1111/1462-2920.14433

Klitgaard-Kristensen, D., Sejrup, H., and Haflidason, H. (2002). Distribution of recent calcareous benthic foraminifera in the northern North Sea and relation to the environment. *Polar Res.* 21, 275–282. doi: 10.1111/j.1751-8369.2002.tb00081.x

Knittel, K., and Boetius, A. (2009). Anaerobic Oxidation of Methane: Progress with an Unknown Process. *Annu. Rev. Microbiol.* 63, 311–334. doi: 10.1146/annurev.micro.61.080706.093130

Korsun, S., and Hald, M. (2000). Seasonal dynamics of benthic foraminifera in a glacially fed fjord of Svalbard, European Arctic. *J. Foraminifer Res.* 30, 251–271.

Kvenvolden, K. A. (1993). Gas hydrates geological perspective and global change. *Rev. Geophys.* 31, 173–187. doi: 10.1029/93RG00268

Levin, L. A. (2005). "Ecology of cold seep sediments: Interactions of fauna with flow, chemistry and microbes," in *Oceanography and Marine Biology: An Annual Review*, eds R. N. Gibson, R. J. A. Atkinson, and J. D. M. Gordon (Boca Raton: CRC Press-Taylor & Francis Group), 1–46.

Loeng, H. (1991). Features of the physical oceanographic conditions of the Barents Sea. *Polar Res.* 10, 5–18. doi: 10.3402/polar.v10i1.6723

Mackensen, A., Wollenburg, J., and Licari, L. (2006). Low $\delta^{13}C$ in tests of live epibenthic and endobenthic foraminifera at a site of active methane seepage. *Paleoceanography* 21, 1–12. doi: 10.1029/2005PA001196

Manley, T. O. (1995). Branching of Atlantic Water within the Greenland-Spitsbergen Passage: An estimate of recirculation. *J. Geophys. Res.* 100, 20627–20634. doi: 10.1029/95JC01251

Martin, J. B., Day, S. A., Rathburn, A. E., Perez, M. E., Mahn, C., and Gieskes, J. (2004). Relationships between the stable isotopic signatures of living and fossil foraminifera in Monterey Bay, California. *Geochem. Geophys. Geosyst.* 5:Q04004. doi: 10.1029/2003GC000629

Martin, R. A., Nesbitt, E. A., and Campbell, K. A. (2010). The effects of anaerobic methane oxidation on benthic foraminiferal assemblages and stable isotopes on the Hikurangi Margin of eastern New Zealand. *Mar. Geol.* 272, 270–284. doi: 10.1016/j.margeo.2009.03.024

Maslin, M., Owen, M., Betts, R., Day, S., Dunkley, J. T., and Ridgwell, A. (2010). Gas hydrates: Past and future geohazard? *Philosoph. Transact. R. Soc. A* 368, 2369–2393. doi: 10.1098/rsta.2010.0065

McCorkle, D. C., Emerson, S. R., and Quay, P. D. (1985). Stable carbon isotopes in marine pore waters. *Earth Planetary Sci. Lett.* 74, 13–26. doi: 10.1016/0012-821X(85)90162-1

McCorkle, D. C., Keigwin, L. D., Corliss, B. H., and Emerson, S. R. (1990). The influence of microhabitats on the carbon isotopic composition of deep-sea benthic foraminifera. *Paleoceanography* 5, 161–185. doi: 10.1029/PA005i002p00161

Millo, C., Sarnthein, M., Erlenkeuser, H., and Frederichs, T. (2005). Methane-driven late Pleistocene δ13C minima and overflow reversals in the southwestern Greenland Sea. *Geology* 33, 873–876. doi: 10.1130/G21790.1

Murray, J. W. (2006). *Ecology and Applications of Benthic Foraminifera*. Cambridge: Cambridge University Press.

Niemann, H., Lösekann, T., de Beer, D., Elvert, M., Nadalig, T., Knittel, K., et al. (2006). Novel microbial communities of the Haakon Mosby mud volcano and their role as a methane sink. *Nature* 443, 854–858. doi: 10.1038/nature05227

Nomaki, H., Heinz, P., Hemleben, C., and Kitazato, H. (2005). Behaviour and response of deep-sea benthic foraminifera to freshly supplied organic matter: A laboratory feeding experiment in microcosm environments. *J. Foraminiferal Res.* 35, 103–113.

Panieri, G. (2006). Foraminiferal response to an active methane seep environment: A case study from the Adriatic Sea. *Mar. Micropaleontol.* 61, 116–130. doi: 10.1016/j.marmicro.2006.05.008

Panieri, G., and Sen Gupta, B. K. (2008). Benthic Foraminifera of the Blake Ridge hydrate mound, Western North Atlantic Ocean. *Mar. Micropaleontol.* 66, 91–102.

Panieri, G., Bünz, S., Fornari, D. J., Escartin, J., Serov, P., Jansson, P., et al. (2017). An integrated view of the methane system in the pockmarks at Vestnesa Ridge, 79°N. *Mar. Geol.* 390, 282–300. doi: 10.1016/j.margeo.2017.06.006

Phrampus, B., and Hornbach, M. (2012). Recent changes to the Gulf Stream causing widespread gas hydrate destabilization. *Nature* 490, 527–530. doi: 10.1038/nature11528

Rathburn, A. E., Levin, L. A., Held, Z., and Lohmann, K. C. (2000). Benthic foraminifera associated with cold methane seeps on the northern California margin: ecology and stable isotopic composition. *Mar. Micropaleontol.* 38, 247–266.

Rathburn, A. E., Pérez, M. E., Martin, J. B., Day, S. A., Mahn, C., Gieskes, J., et al. (2003). Relationships between the distribution and stable isotopic composition of living benthic foraminifera and cold methane seep biogeochemistry in Monterey Bay, California. *Geochem. Geophys. Geosyst.* 4:1106. doi: 10.1029/2003GC000595

Ravelo, A. C., and Hillaire-Marcel, C. (2007). Chapter Eighteen: The Use of Oxygen and Carbon Isotopes of Foraminifera in Paleoceanography. *Dev. Mar. Geol.* 1, 735–764.

Rohling, E. J., and Cooke, S. (1999). "Stable oxygen and carbon isotopes in foraminiferal carbonate shells," in *Modern Foraminifera*, ed. B. K. Sen Gupta (Dordrecht: Springer), doi: 10.1007/0-306-48104-9_14

Rudels, B., Muench, R. D., Gunn, J., Schauer, U., and Friedrich, H. J. (2000). Evolution of the Arctic Ocean boundary current north of the Siberian shelves. *J. Mar. Syst.* 25, 77–99. doi: 10.1016/S0924-7963(00)00009-9

Ruppel, C. D., and Kessler, J. D. (2017). The interaction of climate change and methane hydrates. *Rev. Geophys.* 55, 126–168. doi: 10.1002/2016RG000534

Sahling, H., Rickert, D., Link, P., Suess, E., and Lee, R. W. (2002). Community structure at gas hydrate deposits at the Cascadia convergent margin, NE Pacific. *Mar. Ecol. Prog. Ser.* 231, 121–138. doi: 10.3354/meps231121

Sander, E., and van der Zwaan, B. (2004). Effects of experimentally induced raised levels of organic flux and oxygen depletion on a continental slope benthic foraminiferal community. *Deep Sea Res. Part I Oceanogr. Res. Papers* 51, 1709–1739. doi: 10.1016/j.dsr.2004.06.003

Schneider, A., Crémière, A., Panieri, G., Lepland, A., and Knies, J. (2017). Diagenetic alteration of benthic foraminifera from a methane seep site on Vestnesa Ridge (NW Svalbard). *Deep Sea Res. Part I Oceanogr. Res. Papers* 123, 22–34. doi: 10.1016/j.dsr.2017.03.001

Schönfeld, J., and Numberger, L. (2007). The benthic foraminiferal response to the 2004 spring bloom inthe western Baltic Sea. *Mar. Micropaleontol.* 65, 78–95. doi: 10.1016/j.marmicro.2007.06.003

Seidenkrantz, M. S. (2013). Benthic foraminifera as paleo sea-ice indicators in the subarctic realm - examples from the Labrador Sea-Baffin Bay region. *Q. Sci. Rev.* 79, 135–144. doi: 10.1016/j.quascirev.2013.03.014

Sen, A., Åström, E. K. L., Hong, W.-L., Portnov, A., Waage, M., and Serov, P. (2018). Geophysical and geochemical controls on the megafaunal community of a high Arctic cold seep. *Biogeosciences* 15, 4533–4559.

Serov, P., Vadakkepuliyambatta, S., Mienert, J., Patton, H., Portnov, A. D., Silyakova, A., et al. (2017). Postglacial response of Arctic Ocean gas hydrates to climatic amelioration. *Proc. Natl. Acad. Sci. U S A.* 114, 6215–6220. doi: 10.1073/pnas.1619288114

Smart, C. M., Gooday, A. J., Murray, J. W., and Thomas, E. (1994). A benthic foraminiferal proxy for pulsed organic matter palaeofluxes. *Mar. Micropaleontol.* 23, 89–99.

Smith, L. M., Sachs, J. P., Jennings, A. E., Anderson, D. M., and de Vernal, A. (2001). Light $\delta^{13}C$ events during deglaciation of the East Greenland continental shelf attributed to methane release from gas hydrate. *Geophys. Res. Lett.* 28, 2217–2220. doi: 10.1029/2000GL012627

Stroeve, J. C., Serreze, M. C., Holland, M. M., Kay, J. E., Malanik, J., and Barrett, A. P. (2012). The Arctic's rapidly shrinking sea ice cover: A research synthesis. *Clim. Change* 110, 1005–1027. doi: 10.1007/s10584-011-0101-1

Sztybor, K., and Rasmussen, T. L. (2017). Diagenetic disturbances of marine sedimentary records from methane-influenced environments in the Fram Strait as indications of variation in seep intensity during the last 35 000 years. *Boreas* 46, 212–228.

Torres, M. E., Mix, A. C., Kinports, K., Haley, B., Klinkhammer, G. P., McManus, J., et al. (2003). Is methane venting at the seafloor recorded by $\delta^{13}C$ of benthic foraminifera shells? *Paleoceanography* 18:1062. doi: 10.1029/2002PA000824

Toyofuku, T., Matsuo, M. Y., de Nooijer, L. J., Nagai, Y., Kawada, S., Fujita, K., et al. (2017). Proton pumping accompanies calcification in foraminifera. *Nat. Commun.* 8, 1–6. doi: 10.1038/ncomms14145

Treude, T., Orphan, V., Knittel, K., Gieseke, A., House, C. H., and Boetius, A. (2007). Consumption of methane and CO_2 by methanotrophic microbial mats from gas seeps of the anoxic Black Sea. *Appl. Environ. Microbiol.* 73, 2271–2283. doi: 10.1128/AEM.02685-06

Uchida, M., Shibata, Y., Ohkushi, K., Ahagon, N., and Hoshiba, M. (2004). Episodic methane release events from Last Glacial marginal sediments in the western North Pacific. *Geochem. Geophys. Geosyst.* 5:Q08005. doi: 10.1029/2004GC000699

Walczowski, W., Piechura, J., Osinski, R., and Wieczorek, P. (2005). The West Spitsbergen Current volume and heat transport from synoptic observations in summer. *Deep Sea Res. Part I Oceanogr. Res. Papers* 52, 1374–1391. doi: 10.1016/j.dsr.2005.03.009

Wefer, G., Heinze, P. M., and Berger, W. H. (1994). Clues to ancient methane release. *Nature* 369:282. doi: 10.1038/369282a0

Werner, K., Müller, J., Husum, K., Spielhagen, R. F., Kandiano, E. S., and Polyak, L. (2016). Holocene sea subsurface and surface water masses in the Fram Strait. Comparisons of temperature and sea-ice reconstructions. *Quaternary Sci. Rev.* 147, 194–209. doi: 10.1016/j.quascirev.2015.09.007

Whiticar, M. J. (1999). Carbon and hydrogen isotope systematics of bacterial formation and oxidation of methane. *Chem. Geol.* 161, 291–314. doi: 10.1016/S0009-2541(99)00092-3

Wollenburg, J. E., and Mackensen, A. (1998). Living benthic foraminifers from the central Arctic Ocean: faunal composition, standing stock and diversity. *Mar. Micropaleontol.* 34, 153–185.

Wollenburg, J. E., and Mackensen, A. (2009). The ecology and distribution of benthic foraminifera at the Håkon Mosby mud volcano (SW Barents Sea slope). *Deep Sea Res. Part I Oceanogr. Res. Papers* 56, 1336–1370. doi: 10.1016/j.dsr.2009.02.004

Wollenburg, J. E., Kuhnt, W., and Mackensen, A. (2001). Changes in Arctic Ocean paleoproductivity and hydrography during the last 145 kyr: The benthic foraminiferal record. *Paleoceanography* 16, 65–77. doi: 10.1029/1999PA000454

Wollenburg, J. E., Raitzsch, M., and Tiedemann, R. (2015). Novel high-pressure culture experiments on deep-sea benthic foraminifera — Evidence for methane seepage-related δ13C of Cibicides wuellerstorfi. *Mar. Micropaleontol.* 117, 47–64. doi: 10.1016/j.marmicro.2015.04.003

Yao, H., Hong, W.-L., Panieri, G., Sauer, S., Torres, M. E., Lehmann, M. F., et al. (2019). Fracture-controlled fluid transport supports microbial methane-oxidizing communities at the Vestnesa ridge. *Biogeosciences* 16, 2221–2232.

Zamelczyk, K., Rasmussen, T. L., Husum, K., Godtliebsen, F., and Hald, M. (2014). Surface water conditions and calcium carbonate preservation in the Fram Strait during marine isotope stage 2, 28.8–15.4 kyr. *Paleoceanography* 29, 1–12. doi: 10.1002/2012PA002448

Conflict of Interest: The author declares that the research was conducted in the absence of any commercial or financial relationships that could be construed as a potential conflict of interest.